

PB83-238108

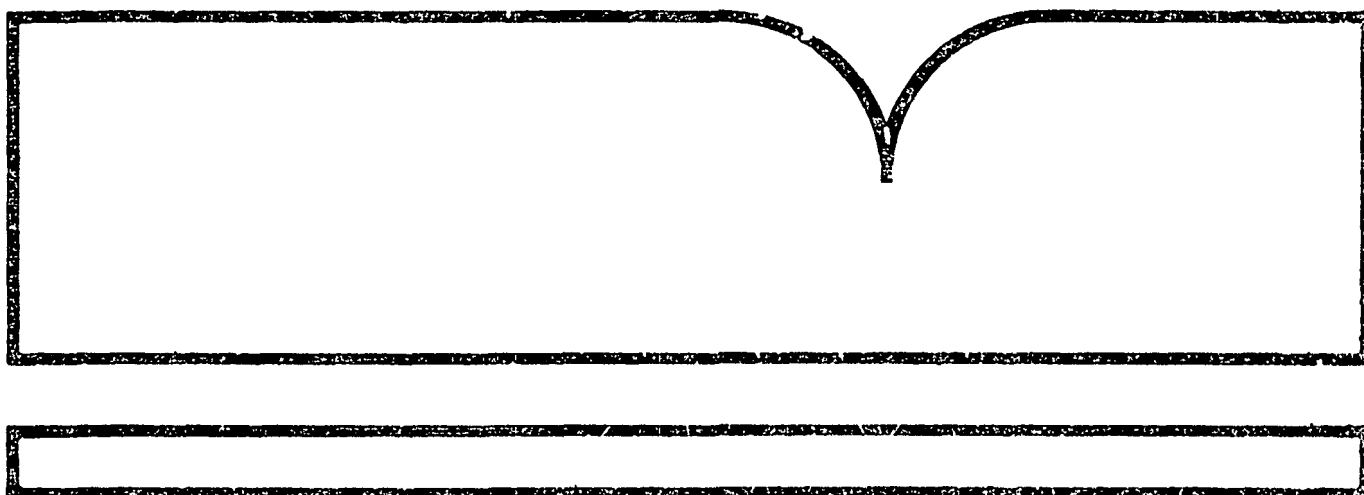
Effects of Suspended Sediments on  
Penetration of Solar Radiation into  
Natural Waters

California Univ., Santa Barbara

Prepared for

Environmental Research Lab., Athens, GA

Jul 83



U.S. Department of Commerce  
National Technical Information Service

**NTIS**

PBBJ-218188

EPA-600/3-83-060

July 1983

EFFECTS OF SUSPENDED SEDIMENTS ON PENETRATION  
OF SOLAR RADIATION INTO NATURAL WATERS

by

Raymond C. Smith<sup>1,2</sup>

Karen S. Baker<sup>2</sup>

J. Benjamin Fahy<sup>1</sup>

<sup>1</sup>Department of Geography  
University of California at Santa Barbara  
Santa Barbara, California 93106

<sup>2</sup>Institute of Marine Resources  
Scripps Institution of Oceanography  
University of California at San Diego  
La Jolla, California 92093

Grant No. 806372019

Project Officer  
Richard G. Zepp  
Environmental Processes Branch  
Environmental Research Laboratory  
Athens, Georgia 30613

ENVIRONMENTAL RESEARCH LABORATORY  
OFFICE OF RESEARCH AND DEVELOPMENT  
U.S. ENVIRONMENTAL PROTECTION AGENCY  
ATHENS, GEORGIA 30613

TECHNICAL REPORT DATA (Please read instructions on the reverse before completing)		
1 REPORT NO EPA-600/3-83-060	2	3 RECIPIENT'S ACCESSION NO 778 3 238188
4 TITLE AND SUBTITLE Effects of Suspended Sediments on Penetration of Solar Radiation into Natural Waters	5 REPORT DATE July 1983	
		6 PERFORMING ORGANIZATION CODE
7 AUTHOR(S) Raymond C. Smith <sup>1,2</sup> , Karen S. Baker <sup>2</sup> , and J. Benjamin Fay <sup>1</sup>	8 PERFORMING ORGANIZATION REPORT NO	
9 PERFORMING ORGANIZATION NAME AND ADDRESS 1 University of California at Santa Barbara, Santa Barbara, CA 93106 2 Scripps Institution of Oceanography, University of California at San Diego, La Jolla, CA 92093	10 PROGRAM ELEMENT NO CCUL1A	
		11 CONTRACT/GRANT NO 806372019
12 SPONSORING AGENCY NAME AND ADDRESS Environmental Research Laboratory--Athens GA Office of Research and Development U.S. Environmental Protection Agency Athens, GA 30613	13 TYPE OF REPORT AND PERIOD COVERED Final, 2/79-12/82	
		14 SPONSORING AGENCY CODE EPA/600/01
15 SUPPLEMENTARY NOTES		
16 ABSTRACT Aquatic photochemical and photobiological processes depend on both the amount and the spectral composition of solar radiation penetrating to depths in natural waters. In turn, the depth of penetration, as a function of wavelength, depends on the dissolved and suspended material in these waters. As a consequence, the rates of photochemical transformation as well as the impact on photobiological processes, depends on the optical properties of these water bodies as determined by their dissolved and suspended material. In particular, because photo-chemical processes are frequently governed by radiation in the ultraviolet region of the spectrum, the optical properties of natural waters in this spectral region are especially important. In this study, several theoretical models were developed and some unique experimental data were developed for the purpose of characterizing the optical properties of various natural waters. Particular emphasis was placed on optical properties in the ultraviolet region of the spectrum. Optical properties of water bodies were modeled in terms of their dissolved materials and suspended sediments so that the solar radiant energy penetrating to depths in these waters can be calculated from available, or easily collected, experimental data. The theoretical models, with input of these data, can then be used to calculate the rates of photochemical and photobiological processes in various aquatic environments.		
17 KEY WORDS AND DOCUMENT ANALYSIS		
a DESCRIPTORS	b IDENTIFIERS/OPEN ENDED TERMS	c COSATI Field/Group
18 DISTRIBUTION STATEMENT RELEASE TO PUBLIC	19 SECURITY CLASS (This Report) UNCLASSIFIED	21 NO OF PAGES 53
	20 SECURITY CLASS (This page) UNCLASSIFIED	22 PRICE

#### DISCLAIMER

Although the research described in this report has been funded wholly or in part by the United States Environmental Protection Agency through Grant No. 806372019 to the University of California at San Diego, it has not been subjected to the Agency's required peer and policy review and therefore does not necessarily reflect the views of the Agency and no official endorsement should be inferred.

## FOREWORD

Environmental protection efforts are increasingly directed towards prevention of adverse health and ecological effects associated with specific compounds of natural or human origin. As part of this Laboratory's research on the occurrence, movement, transformation, impact, and control of environmental contaminants, the Environmental Processes Branch studies the microbiological, chemical, and physico-chemical processes that control the transport, transformation and impact of pollutants in soil and water.

Aquatic photochemical and photobiological processes that affect chemical transformation depend on both the amount and the spectral composition of solar radiation penetrating to depths in natural waters. In turn, the depth of penetration depends on the dissolved and suspended material in these waters. The optical properties of natural waters in the ultraviolet region are especially important. This report describes several theoretical models and some unique experimental data developed for characterizing the optical properties of various natural waters. With these models, the rates of photochemical and photobiological processes in various aquatic environments can be calculated.

William F. Donaldson  
Acting Director  
Environmental Research Laboratory  
Athens, Georgia

## PREFACE

Within an aquatic environment the presence of solar radiation as an energy source is of fundamental importance. Our ability to understand and manage our aquatic resources is therefore strongly linked to our ability to understand the penetration of radiation into a body of water and its apportionment among various components of dissolved and suspended material in the water. This report presents a study in hydrologic optics which included assembling a data base of relevant optical measurements, deriving mathematical models for the solution of the equation of radiative transfer, and deducing from these both simplified theoretical and practical results. This study will have long term benefits, not only to the investigators of hydrologic optics, but also to a wide variety of other fields concerned with understanding and predicting photoprocesses in an aquatic environment.

## ABSTRACT

The relationship between dissolved and suspended constituents in water and the optical properties of a range of water types has been investigated and analytically characterized using several approaches. This characterization permits the spectral radiant energy throughout the water column to be predictively modeled. This in turn provides a basis for the quantitative calculations of photo processes such as photolysis rates, in aquatic environments.

A series of new laboratory experiments has provided a set of data upon which the Bio-optical Component Model (Baker and Smith, 1981) could be further developed. The investigation into the humic acid component has been continued. A new component dealing with a terrigenous clay has been added. Both of these components are parameterized and hence remain within the intended simplicity of the original model.

A brief introduction to underwater modeling is presented as an introduction to the development of a Monte Carlo model. The Bio-optical Component Model allows calculation of the diffuse attenuation coefficient of irradiance, however it does not permit calculations with respect to sun angle or investigations into the changing light field as a function of depth. The Monte Carlo method is a photon tracking technique, essentially a random walk procedure, using the apparent optical properties of the water. This model can then be used to investigate the influences of depth and sun angle on the light field. Technical and practical considerations limit the collection of data pertinent to all light conditions. Indeed, this is the advantage of a model. It can serve as an organizational tool as well as a deductive and predictive tool.

To organize field data to test the developed models, it was first necessary to determine the best available values for the optical properties of the clearest natural waters. An extension and a completion of the set of apparent and inherent optical properties for the clearest natural waters has been described. Also, other optical field data sets have been collected and organized.

This report was submitted in fulfillment of grant #806-372-019 under the sponsorship of the U.S. Environmental Protection Agency. This report covers a period from February 1979 to December 1982 and work was completed as of December 1982.

## TABLE OF CONTENTS

List of Figures.....	vii
List of Tables.....	ix
ACKNOWLEDGMENT.....	
I. INTRODUCTION.....	1
II. CONCLUSIONS.....	4
III. RECOMMENDATIONS.....	5
IV. EXPERIMENTAL.....	7
A. Tank Data.....	7
B. DOM.....	10
C. Other Field Data.....	11
V. THEORETICAL.....	12
A. The Code.....	13
B. Dave Cole.....	13
C. Monte Carlo modeling.....	14
D. POOF.....	15
E. Model Checks.....	16
VI. RESULTS.....	18
A. Atmosphere.....	18
B. Field data - clear water.....	19
C. Field data - tank.....	20
D. Field data - other.....	20
E. POOF model.....	20
REFERENCES.....	41



## LIST OF FIGURES

- Figure 1. Relationships between experimental field data and computer models. 24
- Figure 2. The spectral light attenuation in each of the Clay Group water types #1 - #8 listed in Table 1. 25
- Figure 3. The spectral light attenuation in each of the DOM Group water types #9 - #16 listed in Table 1. 25
- Figure 4. The spectral K<sub>clay</sub> component for each of the Clay Group water types #1 - #8 listed in Table 1. 26
- Figure 5. The K<sub>clay</sub> component for the wavelength range from 275nm to 745nm. 26
- Figure 6. The K<sub>clay</sub> component for the wavelength 550nm for a range of clay [ppm] where the x's are experimental data and the line is a polynomial fit. 27
- Figure 7. The K<sub>clay</sub> component for five wavelengths where 5=300nm, 11=450nm, 13=550nm, and 15=650nm where these points represent data and the solid line is the model fit. 27
- Figure 8. The spectral K<sub>dom</sub> component (with scattering material still present; see text) for a DOM Group water types #11 - #16 listed in Table 1. 28
- Figure 9. The spectral K<sub>dom</sub> component for the DOM Group water types #11 - #16 listed in Table 1. 28
- Figure 10. The K<sub>dom</sub> component for two wavelengths where the points are data and the solid line is a fit. 29
- Figure 11. The spectral (K<sub>dom</sub>+K<sub>clay</sub>) component where the x's are data and the line is the model fit. 29
- Figure 12. The spectral K<sub>tot</sub> data points and analytic model fit as solid lines for the Clay Group. 30
- Figure 13. The spectral K<sub>tot</sub> data points and analytic model fit as solid lines for the DOM Group. 30
- Figure 14. The total scattering b for a variety of water types from molecular scattering to clear water to ocean to river. 31
- Figure 15. The spectral a (solid line), b (dashed line), c (dash dashed line), and b/c (notched line) for SCOR Discoverer station 21 Sargasso Sea waters. The D points are the field data measurements of total diffuse attenuation coefficient whereas the 1,6 are the Monte Carlo calculations of K for 10 degree and 60 degree sun angles. 32
- Figure 16. The a (solid line), b (dashed line), c (dash dashed line), and b/c (notched line) for San Vicente waters. The circled 1,6 points are the field measurements of total diffuse attenuation coefficients for sun angles 10 degrees and 60 degrees whereas the 1,6 points are the Monte Carlo predictions. 33

Figure 17. The particle volume scattering function for fairly clear ocean water (Oceanus cruise station 4) for wavelengths 440nm, 490nm, 520nm, 610nm, and 670nm. 34

Figure 18. The calculated total volume scattering function for very clear ocean water (SCOR Discoverer station 21) for wavelengths 440nm, 490nm, 520nm, 610nm, and 670nm. 35

Figure 19. The Baker-Smith III component model prediction of spectral  $K_{tot}(\lambda)$  for a range of chlorophyll, dissolved organic material and clay. The following explains the composition: 36

line	solid			dashed		dashed dot		hatched	
chl	0	.5	5.	0	0	0	0	.5	5
DOM	0	0	0	.5	5.	0	0	.5	5
clay	0	0	0	0	0	5	25	5	25

Fig. 20. The Monte Carlo calculation of  $K(\lambda, z, 0)$  for wavelength 550nm for sun angles 10, 30, 60, 70, 80 degrees plotted versus optical depths  $cz$  when using only a direct beam input to the water column. 37

Fig. 21. The Monte Carlo calculation of  $K(\lambda, z, 0)$  for wavelength 550nm for sun angles 10, 30, 60, 70, 80 degrees plotted versus optical depths  $cz$  when using both a direct and a diffuse input to the water column. 38

Figure 22. The Monte Carlo calculation of  $K(\lambda, z, 0)$  for clear waters of SCOR Discoverer for sun angle 10 degrees (solid line) and 40 degrees (broken line) for wavelengths 440nm, 490nm, 515nm, and 550nm. The straight line superimposed is the field measured value which is an average for the day. 39

Figure 23. The Monte Carlo calculation of  $K(\lambda, z, 0)$  for San Vicente waters for sun angles 10, 30, 60, 70, 80 degrees for wavelengths 440nm, 550nm, and 670nm. The straight lines superimposed are the field measured values for 10 and 60 degree sun angles. 40

## LIST OF TABLES

Table 1. Tank study water types. 23

#### ACKNOWLEDGEMENT

Richard Zepp recognized the necessity for these studies and acted as project officer during the course of this research. He continually encouraged our research and provided valuable scientific input through informal discussions and the practical utilization of our results. An earlier EPA grant RG806489010, under the BACER program and concerned with the penetration of UV radiation into natural waters, supported the development of the UV spectroradiometer used in this research.

The tank data were obtained with the help of the Marine Applications Group at NASA Langley Research Center, especially Wayne Esaias, Lamont Poole, and Charlie Whitlock - who made the facilities available - and Al Gurganus and Jim Usry who helped obtain the data. Lamont Poole also collaborated in the development of the Monte Carlo modeling. This modeling built upon the earlier work of J.V. Dave and John Kirk.

## SECTION 1

### INTRODUCTION

Aquatic photochemical and photobiological processes depend upon both the amount of solar radiation penetrating to depths in natural waters as well as upon its spectral composition. It is the influence of dissolved and suspended material in the water combined with the characteristics of clear water which determine the attenuation of light in a water column. Our main research objective was to characterize various natural waters, in terms of their constituents and consequent optical properties so that the spectral radiant energy versus depth can be estimated. Waters containing humic acid and suspended sediments were of particular interest. This characterization can then be used to calculate rates of photochemical and photobiological processes in aquatic environments. This in turn allows a quantitative assessment of the photochemical process that may account for the transformation of pollutants in aquatic environments. Some new radiometric laboratory field studies have been made and combined with information from previous bio-optical field studies. This has allowed the further development of models and theory which can in turn be defined and checked by the data.

Preisendorfer (1976) has defined the inherent optical properties of a medium to be those which are independent of the light-field within the water. Included within this set are the beam absorption coefficient  $c$ , the beam scattering coefficient  $b$ , and the total attenuation coefficient  $c$ , where  $c = a + b$ . The parameter  $b$  is actually the integral over all angles of another inherent optical property, the volume scattering coefficient

$$b = \int_{4\pi} \rho(\theta) d\Omega, \quad (1)$$

Preisendorfer has shown the set  $(c, \rho)$  of inherent optical properties to be a sufficient and complete set for describing the optical properties of the optical medium under any circumstances. That is, knowing  $(c, \rho)$ , and an input radiance distribution illuminating the optical medium, which is arranged within some known geometry, one can in principle deduce the resulting radiant flux distribution.

If an optical property does vary with respect to changes in the radiance distribution, it is said to be an apparent optical property. To describe the penetration of solar radiation into natural waters, we use the diffuse attenuation coefficient for irradiance, which is an apparent optical property,

$$K(z, \lambda) = -1/E(z, \lambda) dE(z, \lambda)/dz \quad (2)$$

or alternatively,

$$E(z_2, \lambda) = E(z_1, \lambda) \exp[-K(z, \lambda) \cdot (z_2 - z_1)] \quad (3)$$

where  $K$  has units of reciprocal length,  $z_1$  and  $z_2$  are the depths which increase positively with increasing depth at which  $E(z_1)$  and  $E(z_2)$  are measured. In particular, if the spectral downward irradiance just beneath the water surface,  $E(0, \lambda)$ , and  $K(z, \lambda)$  are known, then the spectral irradiance at

depth,  $z$ , can be calculated.

$$E(z, \lambda) = E(0^-, \lambda) \exp[-K(z, \lambda) \cdot z]. \quad (4)$$

Miller and Zepp (1979) have shown that the average photolysis rate at depth  $z$  and wavelength  $\lambda$  can be expressed by

$$-(dP/dt)_{z, \lambda} = 2.303 \int \phi \cdot \epsilon(\lambda) \cdot E(z, \lambda) \cdot D(z) \cdot [P]_z \cdot d\lambda \quad (5)$$

where  $\phi$  is the quantum yield for the reaction,  $\epsilon$  is the molar absorptivity of the pollutant,  $E(z, \lambda) \cdot D(z)$  is the scalar irradiance at depth  $z$ ,  $D(z)$  is the distribution function at depth  $z$ , and  $[P]_z$  is the pollutant concentration at depth  $z$ . Thus, given the chemical characteristics of the pollutant and its concentration, a knowledge of  $E(z, \lambda)$ , or equivalently  $K(z, \lambda)$ , is sufficient to quantitatively calculate the photolysis rate of the pollutant under consideration.

The diffuse attenuation coefficient is a function of the total attenuation and scattering coefficients. It provides a way of characterizing various natural waters in terms of the dissolved and suspended material in these waters. While the potential for characterizing waters in this way is widely recognized, there are very few data relating the diffuse attenuation coefficient for irradiance to the concentration of suspended material in waters containing relatively high concentrations. The spectral diffuse attenuation coefficient,  $K(z, \lambda)$ , can be expected to be dependent upon the sizes, shapes and concentration of suspended material. Thus, before natural waters of this type can be characterized by an appropriate  $K$ -function, it is necessary to obtain concurrent  $K(z, \lambda)$  and suspended material data.

There are few data available in the ultraviolet portion of the spectrum, the spectral region most critical for modeling photolysis rates. The UV radiation is important for studies of photoreactions because many pollutants absorb sunlight most strongly in this wavelength region. Hence, particular emphasis has been put on collecting data in several water types in the UV region and checking the short wavelength predictions of models.

Modeling has been used to organize data into a classification scheme as well as to permit predictive estimates to be made. Since the diversity of possible water types and of radiant energy geometries is so large, it is necessary to augment data gathering with the development of predictive models which will allow limited data to be extrapolated to situations which have not been defined by a complete set of field measurements.

The component model developed by Smith and Baker (1978a, 1978b, 1982) presents the diffuse attenuation coefficient of irradiance as a function of wavelength defined by water constituents of clear water, chlorophyll and dissolved organic material. This model defines an average  $K_{tot}(\lambda)$  which represents an integrated value of  $K$  to the 1% light level. Tank studies have furthered the development of this model. New information regarding the dissolved organic material has been gathered and a new clay component has been added. The use of this model is enhanced by the fact that it is simple, and

easy to use.

However, a more complete understanding requires models which can be used to predict behavior of light as a function of angle and depth as well as a function of wavelength. Existing radiative transfer theory and variations of Mie scattering theory as well as Monte Carlo modeling have been investigated. This has resulted in the development of a phenomenological model of radiative transfer which permits calculations of upwelling and downwelling radiance and irradiance.

An important test of the limits of such models is comparison with clearest natural waters as well as with turbid waters. Since the clear water optical properties are one of the components of all other water types, it is important to have as complete a set of these properties as possible. The angular scattering and total scattering data for such waters have been incomplete. In the work reported herein these data have been assembled and extended thus completing the set of inherent and apparent optical properties for the clearest waters. When inherent optical properties are input to the Monte Carlo model, it has been shown to reproduce the apparent optical properties. The model is used to extend our knowledge of the behavior of apparent optical properties as a function of wavelength, of depth, and of solar zenith angle.

To simulate realistic and quantitative aquatic light fields, it is necessary to define an input light field to the surface of the water column. This requirement has stimulated research into the effect of varying solar angle and atmospheric conditions on the underwater light field.

Figure 1 summarizes the relationship between the experimental and the theoretical work discussed here. The triangles represent field data. They serve as inputs and checks on the classification schemes and predictive models which are portrayed as boxes. The calculated parameters are represented by circles. In this diagram, the lower dashed area refers to the Balcer-Smith component model of the diffuse attenuation coefficient of irradiance. The upper dashed box describes our Monte Carlo modeling showing its inherent optical property inputs along with the atmospheric lighting geometry,  $L_0$ , input. The output from this model is the apparent optical properties,  $L(\lambda, z, 0)$  and hence  $E(\lambda, z, 0)$  and  $K(\lambda, z, 0)$ . The left hand side of the diagram shows water type constituents whereas the right hand side of the diagram shows the models with their inputs and outputs.

## SECTION 2

### CONCLUSIONS

The organization and further analysis of data has allowed a full suite of inherent and apparent optical properties for clear waters to be deduced. In addition, laboratory investigations of clear water with additions of clay as well as humic acid have allowed the further development of the Bio-optical Component Model. Although this model is simple and easy to use in predicting the light field underwater, it deals only with an average  $K$  and does not permit a further understanding of the underlying processes contribution to light attenuation. The development of the Monte Carlo model has furthered our understanding of both the inherent and the apparent optical properties of natural waters.

The Bio-optical Model III is described by Equation 9. With this model and a knowledge of the chlorophyll, humic acid, and the clay content of a water system, the average diffuse attenuation coefficient for irradiance can be calculated. Given an input irradiance field, it is then possible to estimate the light field at any point in the water column. Having thus defined the environment in terms of the light present, it is possible to investigate various photo processes such as that described by equation 5.

It has been demonstrated that the Monte Carlo model provides closure when applied to the problem of calculating the apparent optical properties of an underwater light field when given the inherent optical properties. Further, by use of the model we have uncovered several important facts. The importance of dealing with the total light field (direct and diffuse) has been discussed and explained. The diffuse attenuation coefficient has been shown to be relatively insensitive to the actual composition of the total light field in terms of the ratio of direct sunlight to diffuse skylight. Further,  $K$  has been found to be only weakly sensitive to the wavelength dependence of the volume scattering function. This has the important consequence that the data from a volume scattering meter at one wavelength may be reliably extrapolated to obtain  $K$  estimates at another wavelength.

By use of the model we have demonstrated, with more completeness than is practical with field data, that the diffuse attenuation coefficient for irradiance will reach an asymptotic value when the averaging effect of depth on the direct and diffuse components begins to take effect. Similarly, it has been shown that there is a significant change in  $K$  as a function of sun angle. This effect is more pronounced in turbid waters than in clearer waters.

The investigations that are summarized are being described in detail in several publications. Manuscripts currently in preparation are summarized in the Appendix.

### SECTION 3

#### RECOMMENDATIONS

The data gathering, description and predictive modeling of environmental processes in practical situations is complex and expensive. The research sponsored here has demonstrated the cost effectiveness of an integrated theoretical and experimental program where limited, but specifically chosen, data have been utilized to test and refine models. These models are in turn utilized to simulate realistic field data for sensitivity analyses and further investigation and predictive modeling of the fundamental processes of interest. Given today's limited resources allocated to the study of important environmental problems, we strongly recommend that the methodology demonstrated in this research program be utilized more frequently.

Our investigations have obtained valuable new data and created theoretical models which will provide solutions to a wide range of environmental problems dealing with natural waters. This work also suggests new directions for further productive research. Specific recommendations include: (1) more complete experimental work in controlled environments (such as tank experiments), especially to obtain the optical properties of important organics and clays and the optical effects when these are mixed; (2) work to increase the speed and efficiency of the Monte Carlo model and the use of this model for continued sensitivity analysis directed toward specific practical problems; (3) the development and application of other solutions of the radiative transfer equation which can be expected to provide increased insight into the fundamental processes underlying practical environmental problems; (4) the use of Mie scattering theory to compute the inherent optical properties (iop) of various natural sediments and the subsequent use of these iop's in our component model to compute the apparent optical properties (aop) for waters of interest.

The quantity and quality of valuable data that was efficiently obtained in our tank experiments demonstrates the usefulness of this approach. New valuable data could be obtained if similar experiments were performed using a range of dissolved organics (especially different humic acids) and different suspended clays and other materials. Future investigations should also include investigation of the effects of the mutual interaction of organic material on the optical properties of water. Such tank experiments are essential in order to define the relationship between optical properties and the constituents of our water systems and for a more complete understanding of photolysis in natural waters.

Considerable value, both for theoretical development and the solution of practical problems, can be obtained from the use and further development of our Monte Carlo model. Increasing the efficiency of the model will proportionally increase its usefulness. Valuable future applications of the model include sensitivity studies of atmospheric parameters influencing the underwater radiant energy distribution; of variability in the volume scattering function, due to chemical and physical modification of suspended particle size and morphology, and how this influences the distribution of radiant energy; of key variables for the purpose of parameterizing the most important effects into simple practical models of photolysis rates; of the scattering and absorption properties of various waters containing representative sediments and how these inherent optical properties effect the distribution function in



these waters.

The usefulness of the Monte Carlo model has also underlined the need for the application of more advanced modeling techniques for some specific optical problems. Monte Carlo models are easily adaptable to a wide range of geometrical configurations of the optical medium. However, they are frequently inefficient compared to more advanced codes. This is especially true for processes where the backscattering plays an important role; i.e., in increasingly turbid waters. In these, and other, circumstances "analytic" models which involve direct solutions of the radiative transfer equation (e.g. spherical harmonics) or which use the operators defined by the interaction principle (e.g. matrix operator models) will usually provide more efficient and accurate solutions. While such models lack the flexibility of the Monte Carlo method, their added effectiveness in dealing with very turbid water situations warrant their further development. In addition, these more advanced models can be expected to enhance our insight into the fundamental processes underlying basic environmental problems concerned with the penetration of radiant energy into natural waters.

Since the diversity and concentration range of possible suspended material is so large, it is necessary to augment data gathering with the development of predictive models which will allow limited data to be extrapolated to unmeasured situations. A particularly valuable approach is to utilize the Mie scattering theory, inputting the relatively large data bases of total suspended and particle size information for natural waters, to calculate the inherent optical properties (iop) for these waters. The iop's can in turn be utilized to calculate the apparent optical properties (aop) and then input to our bio-optical component model for the estimation of radiant energy penetration into these waters.

The "trade-off" between computing power and flexibility has led the authors into the consideration of another approach to the problem of finding one model which is capable of providing both power and flexibility at the same time. It is our conclusion that perhaps the ideal solution lies within the realm of "semi-analytic" models which have the merit of focusing computational power where it is most needed but which still retain the flexibility of being easily adaptable to diverse geometries.

Finally it should be noted that we believe in many cases that investigations which are still in an exploratory stage are best served by approximate methods such as Delta-Eddington approximations. These models provide quick, albeit rough results, which allow the the investigator to determine whether a given path of inquiry is likely to be fruitful. Once an approximate method has been used to determine a basic level feasibility, a Monte Carlo model can be applied to provide extensive theoretical understanding into the nature of the phenomenon of interest. If the results of such an understanding then warrant continued investigation where the utmost efficiency and accuracy is required, either a matrix operator, spherical harmonic, or similar analytic method, should be specifically adapted to solve the problem more rigorously.

## SECTION 4

### EXPERIMENTAL

Considerable work has been done in the past using optical instruments in aquatic field work. However, as waters become more turbid (hence often more complex and variable), a more controlled investigation of the water types is warranted. Several optical studies of turbid waters simulated in a defined tank environment have been carried out. This information, in addition to our own previous optical data base as well as the data base of colleagues who have worked in more turbid river environments, has yielded a relatively complete picture of the optical properties for a broad range of water types.

#### TANK DATA

Known amounts of dissolved organic material (DOM) and terrigenous material (clay) were added to a tank of filtered water while the optical properties were continually monitored. These data may be used then to describe the influence of each substance individually on the attenuation of radiant energy in water. A further analysis yields possible parameterizations of each attenuating component. This series of experiments was run using the Langley Research Center tank facility and solar simulator.

The tank facility consists of an enclosed laboratory, the tank and associated filtering and pumping capabilities, and a solar simulator. The tank is a stainless steel cylinder painted black on the inside. The diameter is 2.4 meters; the depth is 3 meters; the volume is approximately 11,600 liters. Since the measurements used were relative, the absolute spectral output of the solar simulator was not critical. However, because the simulator had a high UV output, optical data could be obtained in this spectral region which would otherwise have been impractical under natural conditions.

The organic material added came from the Aldrich Chemical Company. It was listed as a humic acid with catalog H1, 675-2 in crystalline form. These crystals were dissolved in filtered deionized water before adding the tank water. The terrigenous material added was a calvert clay which in powdered form had a reddish tinge characteristic of some soil sites in the eastern United States. A summary of all water types created is given in Table 1. Note that measurements #1 and #9 represent "clear" filtered water and are thus referred to as base line measurements. There are essentially two groups represented here: the Clay Group, where successive additions of clay are made to the water, and the DOM group, where successive additions of DOM are made to the water. These data have been summarized in Figures 2 and 3 where the total diffuse attenuation coefficient for irradiance is plotted as a function of wavelength for the two groups.

Transmittance measurements during each water type investigation indicated that the simulated environment in the tank remained relatively stable. The water was being mixed at intervals in order to maintain this uniformity. A complete description of the data and its analysis will be given in an SIO report (Baker, in preparation).

The main optical measurements made included spectral irradiance at a series of ten depths using the submersible spectroradiometer (Smith et al.

1979) capable of measuring at any chosen wavelength in the range from 270 nanometers to 750 nanometers. This instrument has a 1 nm full width at half max pass band and was designed specifically to enable accurate underwater measurements in the ultraviolet region to be made.

The component model defines

$$K_{tot}(\lambda) = (1/z_{max}) \int_0^{z_{max}} K(z, \lambda) dz \quad (6)$$

where  $z_{max}$  is the 1% light level. Equation (4) reduces to

$$K_{tot}(\lambda) = (-1/z_{max}) * \ln[E(z_{max}, \lambda)/E_0(0, \lambda)] \quad (7)$$

Thus from the  $E(\lambda)$  versus depth measurements, a total diffuse attenuation coefficient may be calculated by making a linear least squares fit through the data.

The spectral diffuse attenuation coefficient for the irradiance can be partitioned into components:

$$K_{tot}(\lambda) = K_w(\lambda) + K_c(\lambda) + K_t(\lambda) \quad (8)$$

where  $K_w(\lambda)$  is the attenuation due to pure seawater,  $K_c(\lambda)$  is the attenuation due to chlorophyll,  $K_d(\lambda)$  is the attenuation due to DOM and  $K_t(\lambda)$  is the attenuation due to terrigenous material. The  $K_w$  component has been measured and discussed previously (Smith and Baker, 1981; Baker and Smith, 1982). The  $K_c$  component has been parameterized based upon extensive field data (Smith and Baker, 1978a,b; Baker and Smith, 1982). DOM component investigations have been carried out based upon spectral irradiance field measurements (Baker and Smith, 1982) which were limited due to lack of quantitative bio-chemical measurements of the DOM present. And finally, the  $K_t$  component has not been investigated previously by these authors. The present data set permits investigation into the  $K_d(\lambda)$  and  $K_t(\lambda)$  components.

Equation 8 will be written for this work

$$K_{tot}(\lambda) = K_w(\lambda) + K_c(\lambda) + K_{clay}(\lambda) \quad (9)$$

in order to emphasize that the terrigenous component investigated consists of only one type of clay. Until further such studies are completed, one can not be sure what the influence of different terrigenous materials will be on the light attenuation.

In the Clay Group of measurements made, we may assume that  $K_c(\lambda) = 0$  and the  $K_d(\lambda) = 0$ . Any attenuating substances that are present in the initial filtered water are thus lumped into the  $K_w(\lambda)$  base line measurement:

$$K_{clay}(\lambda) = K_{tot}(\lambda) - K_w(\lambda) \quad (10)$$

Thus the K<sub>clay</sub> component for measurements #2 through #8 of Table 1 can be calculated. A plot for the resultant clay component is shown in Figure 4. This component can be written

$$K_{clay}(\lambda) = k_{clay}(\lambda) * T \quad (11)$$

where  $k_{clay}(\lambda)$  is the specific attenuation coefficient of irradiance due to clay and T is the measure of clay particles in parts per million [ppm]. Figure 5 plots this data for all wavelengths in the range from 275 nm to 745 nm as a function of the amount of clay present. To look in more detail, the wavelength 550 nm is shown in Figure 6 where the actual data points are given as x's. The form of this curve suggests a polynomial fit of the form:

$$K_{clay}(\lambda) = (B(\lambda) + C(\lambda) * T) * T \quad (12)$$

This fit is forced through the origin in order to conform to the reality that when there is no terrigenous material present, there can be no attenuation due to the terrigenous component. When such a fit is made, the resulting  $C(\lambda)$  is found to be relatively constant such that

$$C(\lambda) = -.0043 \quad (13)$$

which is wavelength independent. When this assumption is presumed true, a new linear least squares regression can be made to obtain a new set of  $B(\lambda)$ . This parameter can be described by a line fit:

$$B(\lambda) = A + B * (\lambda) \quad (14)$$

where a linear least squared fit yields

$$\begin{aligned} A &= .408 \\ B &= -.000317. \end{aligned}$$

In summary, this gives

$$K_{clay}(\lambda) = [.408 -.000317 * (\lambda)] * T -.0043 * T * T \quad (15)$$

where  $k_{clay} = (.408 -.000317 * (\lambda) -.0043) * T$  which is the specific attenuation coefficient for this clay. To indicate the accuracy of this fit, Figure 7 shows the original data as points and the parameterized fit as a solid line. Because of the nature of the data, an inverse wavelength dependence was also investigated in order to see whether a better fit could be obtained. Using a technique similar to that described above, it was found that

$$K_{clay}(\lambda) = [.119 -.201 * (\lambda/\lambda_0)^{-1}] * T -.0043 * T * T \quad (16)$$

where  $\lambda_0 = 375$  in this case. This parameterization did not improve the fit to the data.

## DOM

Note that the DOM Group contains what might be called two sets of on-line measurements. The #9 in Table 1 is the filtered clear water case. However, a small amount of clay has been added to all DOM waters in order to increase the light absorption and thus decrease the possible influence of the tank walls. The diameter of the tank is approximately 1.2 meters. The instrument was no longer visible at 1.2 m when 6.47 ppm was in the water. Thus the amount of clay added was chosen to be the #4 case of the Clay Group.

The  $K_{dom}$  component can be calculated

$$K_{dom}(\lambda) = K_{tot}(\lambda) - [K_w(\lambda) + K_{clay}(\lambda)] \quad (17)$$

where the case #10 in Table 1 is taken to represent  $K_w + K_{clay}$  for the DOM Group of water types. The plot of the DOM components is shown in Figure 8. Previous workers have investigated the DOM absorption and have always found that the absorption approaches zero as the 650 nm wavelength is reached. This certainly is not the case with the curves in Figure 8. Instead, these curves would lead one to believe that there is a scattering agent present in the humic acid added to the water. This in fact agrees with observations from other investigators who have used similar sources of  $LO^4$  (Zepp, private communication). If we assume that this scattering agent has a behavior similar to that of the clay component discussed above, we can calculate what the amount  $T[ppm]$ , must be. This is done by assuming that  $K_d(650) = 0$ , thus

$$K_{clay}(650) = K_{tot}(650) - K_w(650) \quad (18)$$

Given this value of  $K_{clay}(650)$ , one can then solve equation 15 for  $T$ . When this  $T$  is then used to calculate an additional  $K_{clay}(\lambda)$  term which can then be subtracted in order to give the true  $K_{dom}(\lambda)$ . The resulting  $K_{dom}(\lambda)$  curves are shown in Figure 9.

The form of the  $K_{dom}$  component is

$$K_{dom}(\lambda) = k_o(\lambda_o) * D \exp[(-k_d') * (\lambda - \lambda_o)] \quad (19)$$

where  $\lambda_o$  can be chosen as desired. At the  $\lambda_o$  wavelength,

$$K_{dom}(\lambda) = k_o(\lambda_o) * D \quad (20)$$

so that  $k_o(\lambda_o)$  can be obtained making a linear least squares fit as is shown in Figure 10 for the two cases 375 nm and 450 nm. The fit is again forced through the origin. For the case of 375 nm the slope and therefore  $k_o(\lambda_o)$  has been found to be 1.544; for the  $\lambda_o = 450nm$  case,  $k_o(\lambda_o)$  has been found to be 0.804. This latter value is in the range found by R.G. Zepp (1981) for a similar DOM substance. It was found in ocean field work (Smith and Baker, 1982) that  $k_o(\lambda_o) = 0.565 (1/m)(mgDOM/l)$ . With this identification of  $k_o(\lambda)$ , Equation 19 may be reformed as

$$\ln[K_{dom}(\lambda)/K_0(\lambda_0)*D] = kd'(\lambda-\lambda_0). \quad (21)$$

Solving this equation with a linear least squares fit through the origin gives a slope of  $kd' = -.0104$  which is found to be relatively wavelength independent. This is exactly the value for the slope found by Zepp (1981) in his laboratory work. It has been found with ocean field data (Baker and Smith, 1982) that  $kd'$  ranges from  $-.014$  to  $-.020$ .

This then gives us a defined component for the Aldrich humic acid

$$K_{dom}(\lambda) = D * 1.54 * \exp[-.0104*(\lambda-375)]. \quad (22)$$

The extent to which this reproduces the original data is shown in Figur. 11 where the points are the actual data and the solid line is derived from equation 22 with the appropriate D.

A final look at the fit of the analytic model to the experimental data is shown in Figures 12 and 13 where the total attenuation coefficient  $K(\lambda)$  is plotted versus wavelength. The x's represent actual data while the solid line is the model prediction.

#### OTHER FIELD DATA

The data collected by Smith and others at the Visibility Laboratory at Scripps Institution of Oceanography covered a wide range of oceanic water types. Measurements made in a local reservoir helped extend the turbid water types. At the NASA Langley research center, instruments have been developed for the express purpose of measuring optical properties in turbid waters. Through collaboration with this group, an extensive set of data for a wider range of water types was available for our modeling studies. Figure 14 gives a sampling of this data from very clear waters to quite turbid waters.

## SECTION 5

### THEORETICAL

Modeling has played, and will continue to play, an important role in the understanding and prediction of spectral radiation behavior underwater. This is because field data is difficult and relatively expensive to obtain. Also once a working model exists, it can be used to extend and extrapolate the necessarily limited field data sets. Use of the models also permits one to investigate problems that are particularly difficult in the field (i.e., low sun angles or great depths), and to investigate unsampled water types, to simulate variations in  $b/c$  or  $\mu$ , and to do general sensitivity studies. Such modeling helps verify our understanding of sub-microscopic processes and provides an important theoretical link between the constituents of an optical medium and its resultant optical properties.

Much of radiative transfer modeling has been concerned with the atmosphere. An excellent summary of atmospheric work is given by the IAMAP Radiation Commission (1977). These models were studied to determine their adaptability to our needs for a flexible yet accurate solution to the problem of propagation of radiation within a variety of aquatic environments.

Atmospheric models may be classified in several ways. For instance, a few methods are summarized here with notes included to briefly mention some of the investigators using the techniques. It is mentioned whether the investigator has worked on the method in the past, has a currently working model, or is developing it now.

#### Exact Analytic Methods

1. Singular Eigenfunction method
2. Wiener-Hopf technique

#### Computational Analytic Methods

1. Spherical Harmonics (Dave now)
2. Matrix Operator method (Plass-Kattawar now, Gordon now)
3. Doubling or adding method (Herring, Fitch)
4. Iteration Methods (Dave past)

#### Computational ("non-analytic") Methods

1. Monte Carlo (Plass-Kattawar past, Gordon past, Kirk, Fahy-Poole)
2. Successive Orders of Scattering or natural solution (Preisendorfer).

#### Approximate Methods

1. Eddington approximations (Delta-Eddington)
2. single scattering - approximate Monte Carlo (Gordon past)
3. two stream approximations
4. approximate diffusion theories

The above list is by no means complete but does mention the models we have devoted the most time to exploring, and which appear to be receiving the most attention in the literature. It should be noted that the approximate methods usually yield only an irradiance solution whereas the others give

radiance solutions. Our investigation of computational methods focused on Dave's code for an iterative solution and a Monte Carlo code adapted from Kirk which had the added virtue of being a water model rather than an atmospheric model. Both of these codes were extensively modified to suit our purposes: the Dave code because it did not directly apply to aquatic media and the Kirk code because it was comparatively inefficient. It should be recognized that despite the adaptability of the Monte Carlo code to the demands of aquatic geometry, the spherical harmonics and matrix operator methods are more efficient in terms of computation time.

We have also utilized the solution to the Mie scattering of light with which we can deduce the inherent optical properties from particle size of suspended sediments. This in turn can be used as inputs to either of the above two models. An overview of our modeling to date is summarized in Figure 1.

#### MIE CODE

Mie scattering theory represents an analytic solution of the scattering of light by small spherical particles. The solution due to Mie dates back to the turn of the century and relies solely on Maxwell's discovery that light may be represented in terms of corresponding electric and magnetic fields. Given a spherical particle of a given index of refraction, one may calculate the absorbing and scattering effects of that particle. Given a distribution of such particles, one may build up a model of the particular components of absorption and scattering, within an optical medium of interest. If other components of absorption and scattering due to such factors as chlorophyll or dissolved organic material are known, then the total absorption and scattering coefficients can be deduced. Hence we postulate this code could be an effective underwater technique. The Mie code allows one to arrive at the inherent optical properties of an optical medium by making measurements which are not optical in nature.

The code as obtained from Dave (programs SPA, SPB) did not take advantage of some recent developments in calculating various subparameters. Mie scattering calculations are extensive in time owing to their inherent instabilities. Great care must be taken in insuring computational accuracy to extended precision, e.g., out to 14 places. Wiscombe (1979) has put out a useful note recommending a number of ways to increase efficiency of calculation, and these suggestions were incorporated into the Dave code. In addition certain portions were extracted for calculation via a Floating Point Systems 120b Array Processor, which added a further computational advantage over the original code. These programs were tested against the data of other researchers and reasonable results were obtained. This program set is presently running on both an IBM 360 and on a PRIME 550, 750.

#### DAVE CODE

Code by Dave (1972) existed to provide a direct iterative solution to the radiative transfer equation within an atmospheric context under the assumption of a Lambertian Gound layer. Various inputs were required, including a table of pressures versus heights, aerosol distributions, ozone concentrations, and



the Rayleigh-scattering optical depth of the atmosphere. This code was modified so that the bottom was made Fresnel, which is appropriate for an aquatic interface. The changes required were not trivial since the Dave code had partitioned photons into unreflected and reflected histories, and for reflected photons used the Lambertian assumption to remove the azimuthal dependence of the reflected radiance. The objective in modifying this code was to use it to obtain accurate input radiance distributions to a water model which would then be able to calculate the desired optical properties within the water column. The separation of the atmosphere/ocean problem into first an atmosphere and then a water problem requires the assumption that photons which backscatter from water to air and back into the water represent a negligible contribution to the flux received by the water. The functional layout of the Dave code was presented in a previous report (Interim Progress Report, EPA Grant #806-372-010), and thus it will not be repeated here. This converted version of the Dave code for the atmosphere was running on the IBM 360.

#### MONTE CARLO MODELING

Because the Dave code requires inputs which are not routine measurements for most investigators, an alternative modeling approach was followed in parallel with the modification of the Dave Code. This alternative approach was to pursue the development of a Monte Carlo procedure which would use as inputs the inherent optical properties which had been measured previously by our group; and whose outputs, or "predictions", could be checked against a corresponding set of apparent optical properties also available from earlier studies.

Monte Carlo solutions for the atmosphere-ocean system were reported in the literature in 1969 by Plass and Kattawar. The Monte Carlo method is fundamentally less accurate than the analytic methods but was among the first to be adapted to an atmosphere-ocean system because of its flexibility. The early calculations were restricted to sun positions directly overhead and input phase functions were calculated from Rayleigh and Mie scattering theory. Over time, solutions have been carried out by several authors under a wide variety of conditions (Plass and Kattawar, 1969; Gordon, 1975, 1977; Kirk, 1981). Indications of the power of such simulations have been demonstrated in the form of papers which propose empirical relations between the inherent and apparent optical properties, as derived via Monte Carlo exploration (Gordon *et al.*, 1975; Kirk, 1981). Yet due to problems strictly associated with obtaining sufficiently complete data sets, none of these authors have been able to confirm the model within a comprehensive set of water types as found within nature.

Briefly, a Monte Carlo technique is a "random walk" procedure in which a computer simulates and keeps track of the path of a large number of individual photons as they scatter through, and are eventually absorbed by, the optical medium. It is the set of inherent optical properties of the water, i.e.,  $a$ ,  $b$ , and  $\beta$ , which define the probabilities of events, i.e., scattering and absorption, within a given photon's "life history". Thus the input to the Kirk code was exactly what we were looking for: the inherent optical properties of the water.

The meaning of the term "large number of photons" is defined operationally. As with any statistical sampling procedure involving the average of a measured quantity over many trials, the variance of the output decreases with the number of samples. Thus, for example, perfectly smooth curves of  $K$  versus depth are expected if an infinite number of photons are run. If less photons are run, less than perfectly smooth curves are obtained. In practice a large number of photons are run and the resultant curves examined. If the curves are not considered smooth enough, more photons are run. The number required to achieve some arbitrary standard of "smoothness" is a function of the ratio of absorption to scattering as well as of the optical property being estimated. High absorption will generally require more photons to get the same smoothness, and upwelling properties will almost always require many more photons than their downwelling counterparts. Thus the number of photons required to get good estimates of a given parameter may be anything from a few tens of thousands up to the hundreds of thousands. One can understand that an iterative solution of the equations of radiative transfer, such as used by Dave, is inherently more accurate than the Monte Carlo type solution since it is an exact solution.

A copy of Kirk's Monte Carlo procedure was gratefully obtained from Dr. Kirk and modified. The Kirk Monte Carlo code is running on a Prime 550, 750. The results were checked against Kirk's, and were found to agree.

#### POOF

It was decided that the Monte Carlo technique was an appropriate method to investigate further the attenuation of light underwater. However, it was found necessary to make major alterations to the original Kirk code in order to improve computational efficiency. Further, the original Kirk code approximated the input radiance distribution as a delta function, which is appropriate for sun high in the sky but which is known to be a poor approximation for low sun. After considerable improvements had been made, we cooperated with another researcher in the field (Poole, 1982) in order to produce an efficient, state-of-the-art Monte Carlo code. This code is a significant improvement upon the original code and is detailed elsewhere (Fahy and Poole, in preparation). It is named POOF after its authors (Poole and Fahy).

POOF uses an important approximation of the input radiance distribution by approximating it as a delta function plus a diffuse "skylight" component. The method by which it incorporates data measured in the field to produce a representative input distribution is discussed below, in the results section.

A severe problem with the Kirk model was the number of photons required as input at the surface in order to obtain a usable number at depths below a few attenuation lengths. A photon was highly unlikely to survive long enough before absorption to reach significant depths. To address this problem photons were given statistical weights which are decremented at each interaction with the medium. The decrement factor is simply  $b/c$ , which gives the probability of scattering (i.e., surviving) instead of absorbing in a given interaction. Thus, a photon does not perish by being absorbed but rather, lives on, albeit with a lower weight than before. Eventually the weight of the photon becomes insignificant and the photon is discarded and a new photon is sent on its way.

Other improvements fall under the category of precalculating information that is needed repeatedly. For instance at every collision the collection "bins" in which a photon belongs must be updated. Where the photon belongs typically involves taking an arcsin or arccos, which is a lengthy computation. But since we know in advance which bins correspond to which cosines, it is possible to pre-calculate a mapping from the direction cosines of the photon (which describe its direction) to the bin in which it belongs. This saves considerable time. Another example is the method by which a scattering angle is determined. It involves sampling from a uniform random variable and then doing a table look-up to get a corresponding angle. But the table look-up procedure may be represented as a mapping which can also be precalculated. A table look-up can thus be reduced to sampling within a linear array, the elements of which correspond to values of the uniform random variable.

The most significant improvement of POOF over previous efforts is its partitioning of the problem into two separate "phases"; the first of which depends only on the volume scattering function, and the second, which uses the output of the first, and the remaining input (a,b) to obtain the final solution. The product of the first phase is a series of count arrays, which in a very real sense contain the same sort of information as is calculated by the so-called Natural Solution of radiative transfer, also known as the Successive Orders of Scattering Solution. Thus, POOF may accurately be called a combination of Monte Carlo and Successive Scattering methods.

By dividing the solution into two stages, it is possible to test the sensitivity of the final results to the various input parameters in a particularly straight-forward fashion. Whereas other models require simultaneous input of ( $\mu$ , a, and b), POOF requires  $\mu$  only in the first phase and then (a,b) in the second phase. Since the second phase is extremely short (a few minutes of CPU time) it is possible to obtain an entire set of  $\mu$ , (a,b) combinations in little more time than it takes to compute one  $\mu$ , (a,b) combination. Further, it was found within a given water type, that the wavelength of the selected for the first stage only weakly affected the final results. Thus it now appears possible to select a  $\mu$  within the mid-range of a group of wavelengths of interest, run the first stage just once for this  $\mu$ , and then run the second stage on a full suite of (a,b) pairs corresponding to all the wavelengths desired. Inasmuch as other methods require running each combination individually, this is a substantial savings when one is interested in a full spectrum of predictions.

The POOF model has been compared against data and agrees extremely well with the measurements of the downwelling attenuation coefficient of irradiance as a function of depth. The upwelling radiance and hence upwelling diffuse attenuation coefficient calculations need further investigation to resolve the disparity between model and measurements. It is not surprising that there are problems in this area due to the fewer number of photons upwelled, and hence the increased sensitivity of the model in such situations, to the effects of stochastic noise.

#### MODEL CHECKS

The validity of a theoretical model is best checked by comparing its results with field measurements near the limits of its range of applicability.

Hence, we will show here a comparison of the Monte Carlo results with both clear water field measurements and San Vicente field measurements which are a more turbid water type. The reservoir is representative of more productive waters having a chlorophyll concentration of approximately 7 mg chl/m<sup>3</sup> and an attenuation length of 1/3 meter.

The consistency of the model's predictions with values of K measured in clear waters is demonstrated by Figure 15. Plotted versus wavelength are several inherent and apparent optical properties of the water. Also plotted are the model's predictions of the value of K at one optical depth for zenith angles 10 and 60 degrees (labeled '1' and '6', respectively), along with the measured values of K from the cruise data. Note that the values over the water column, because technical difficulties made it impossible to measure an instantaneous value of K at any given depth. Further, the K's obtained from the data represent averages over sun angle, since measurements were taken slowly compared to the movement of the sun. With these limitations of the cruise data in mind, one sees that the model compares extremely well with the field data, which in every case fall between the 10 degree and 60 degree predictions. This is to be expected since measurements were only taken for a range of sun angles within these limits.

The consistency of the model's predictions for a more turbid water is shown in Figure 16. In this figure the dashed lines give the predicted (model) values of average attenuation coefficient over the first seven meters obtained by fitting a straight line to the log of the irradiance predictions given by the model. The solid lines give the values obtained in a similar manner from the data. Note the wide variance in values of K over wavelength, and the ability of the model to track this variance, even the turn-around wavelength of minimal K, 550 nm.

## SECTION 6

### RESULTS

The results of this work can be broken into several related sections. First a consideration of atmospheric influences of light was made. The input irradiance affects the underwater light field and thus affects both the field data and the modeling of such data. Next, the field data needed was taken and/or analyzed, including specifically an investigation of clear water scattering, of clay and DOM attenuation from a series of tank experiments, and of the suite of data with complete sets of inherent optical properties available. Finally, the results of the Monte Carlo Model, which involves knowledge both of the atmosphere and of the field data, are given.

#### ATMOSPHERE

In developing models of aquatic environments, one must first consider the input radiance distribution. We have considered two quite different approaches; an analytic approach and an experimental approach. The analytic method is that of Dave, an iterative solution to radiative transfer equations discussed earlier. This code has the advantage that it allows definition of the atmosphere based on its constituents.

The second technique involves definition of the input radiance distribution as a delta function plus a uniform diffuse component. This however is a crude approximation of the sky component. In fact, the Dave code will serve as a useful check of the validity of this distribution assumption since the Dave code gives an "exact solution". However, the field data available describes a sky and a direct beam, hence the emphasis on the experimental approach.

The total atmospheric radiation at the water surface may be approximated as a direct solar beam plus a diffuse sky component.

$$E_{tot}(0, \lambda) = E_{direct} + E_{sky} \quad (23)$$

It is possible to measure  $E_{sky}$  and  $E_{tot}$  in the field. It is the ratio of these quantities

$$y = E_{sky}/E_{tot}$$

that the model uses to approximate an input radiance distribution. It is possible to pick an arbitrary  $E_{sky}$  and then to calculate

$$E_{direct} = (1-y) * E_{tot} = (1-y) * (E_{sky}/y) \quad (24)$$

We then integrate  $E_{sky}$  using a uniform radiance and add this to  $E_{direct}$  and propagate through the surface using Fresnel transmittance.

Field measurements of  $y$  in both an oceanic atmosphere as well as in a desert-like atmosphere have been made. These measurements were available only for wavelengths above 400 nm. Using another model (Green *et al.*, 1976; Baker *et al.*, 1981), this data can be extended to the 280 nm region. Using both of these sets of data as surface irradiance input to the Monte Carlo model, the influence of two very different atmospheres could be detected.

#### FIELD DATA - clear water

The measurements in the clearest natural waters of the inherent and the apparent optical properties are limited. As a result, we combine data from the laboratory with data from the field. Our objective is to obtain a data set representative of the clearest waters one might expect to find naturally in the environment.

The most recent and most reliable data of the total absorption coefficient of pure water,  $a_w(\lambda)$  in the 200-800 nm spectral region are summarized in Table 1 (from Smith and Baker, 1981). There is no such information regarding the scattering of clear water. The total volume scattering function can be described as composed of two components, one due to molecular scattering of pure sea water,  $\mu_m$ , and one due to all other components which we will refer to as "particles",  $\mu_p$ .

$$\rho(\theta, \lambda) = \mu_m(\theta, \lambda) + \mu_p(\theta, \lambda) \quad (25)$$

where Morel has shown

$$\mu_m(\theta, \lambda) = b_m(\lambda)/16.06 * (1 + .84 \cos^2(\theta)) \quad (26)$$

The molecular scattering of clear water,  $b_m(\lambda)$  is given elsewhere (Smith and Baker, 1981).

A comparison of all currently available clear water scattering measurements has shown that the SCOR Discoverer Station 21 data (1973) is the most accurate and representative measurement of  $\rho(\lambda)$  for the clear waters. This station was in the Sargasso Sea which is recognized to be among the clearest of ocean waters. Since the scattering data in this set exists only for the wavelength 515 nm, it is necessary to find an extrapolation technique to obtain  $\rho(\theta)$  at other wavelengths. The volume scattering function at the wavelengths 440, 490, 520, and 670 nm, exists for the Oceanus Station 4 data, as is shown in Figure 17, where the molecular scattering has been removed. A very simple method which is consistent with a "diluted water" treatment, assuming that the data sets dealt with are essentially the same water type, has been adopted. Suppose we have two water samples, the second of which is a simple dilution of the first. Thus the first sample has an instantaneous particle size distribution of  $N_1(D)$ , and the second has a distribution  $N_2(D)$ , where  $D$  refers to particle diameter. Then

$$N_2(D) = K_{21} * N_1(D) \quad (27)$$

where  $K_{21}$  is a constant which does not depend on  $D$ . Let  $\mu(\lambda, D, \theta)$  be the scattering due to a particle of diameter  $D$ , in direction  $\theta$ , at wavelength  $\lambda$ . Then

$$d\mu_{p1}(\lambda, \theta) = \mu(\lambda, D, \theta) * N_1(D) dD \quad (28)$$

and it can be shown

$$\mu_{p2}(\lambda, \theta) = K_{21} * \mu_{p1}(\lambda, \theta) \quad (29)$$

Since this result is wavelength independent, we can use it to extrapolate the water dependence of water sample 2 to water sample 1 by

$$\mu_{p1}(\lambda, \theta) = \mu_{p1}(\lambda_0, \theta) * H(\theta) \quad (30)$$

where

$$H(\theta) = \mu_{p2}(\lambda_0, \theta) / \mu_{p1}(\lambda_0, \theta) \quad (31)$$

Given the similarity of water samples taken on these two cruises, we felt the diluted solution approximation to be a reasonable approximation. The validity of this technique was checked using several other complete data sets. Hence the extrapolation from one data set to the next could be checked since the second set of measurements had been made. When such comparisons were made between similar water types, the method produced very accurate reproductions. Given Equation 30, we can now calculate the volume scattering function for other wavelengths for clear water as is shown in Figure 18.

#### FIELD DATA - tank

Figure 19 shows what the Baker-Smith component model gives for a range of  $C$ ,  $D$ , and  $\Gamma$  values. The experimental component analysis has thus yielded not only a description of a set of water types, but the ability to generate a range of water types based upon a choice of eulrophyll, DOM, and clay.

#### FIELD DATA - other

All of the field measurements of scattering must be integrated over all angles to yield a total volume scattering function. This was done using a program designed to take into account the geometry of the scattering instrument used (Petzold, 1972). This program was converted to the PRIME 750, 550, from an IBM 360.

#### POOF MODEL

The limitation of cruise data is that the values of  $K$  usually represent averages over depth and sun angle due to changing light and water conditions.

The model is not confined by such problems and thus it becomes possible to look in detail at the variation of the apparent optical properties with sun angle and with depth.

Figures 20 and 21 demonstrate a need to include a sky component in modeling calculations. The graphs of  $K_d$ , the downwelling diffuse attenuation coefficient, show a much greater variance with solar zenith angle for a model using input of a direct beam only, than is evidenced in the POOF calculation. Direct comparisons for solar zenith angles of 5 to 35 degrees show little difference between the two models while the models differ significantly for solar zenith angles of 75 to 85 degrees. Of particular interest is the reversal of order of the vertical positioning of the 70 and 80 degree curves in Figure 16. For the direct beam model, the 80 degree curve lies above the 70 degree curve, while for POOF the 80 degree curve is less extreme than the 70 degree curve. This is because in POOF, the model takes into account that almost all the input into the water for the 80 degree curve is diffuse skylight, the Fresnel transmittance through the water at 80 degrees zenith angle being extremely low. The general pattern of light entering the water therefore, closely resembles the diffuse skylight, which represents something of an average of the direct beam results for solar zenith angles from 0 to 90 degrees.

Notice that the values for  $K$  in these figures for 80 degrees are less extreme than are the values for the 60 degree curve. It can be shown that  $K$  increases with theta until a theta-max at which point it decreases since an averaging effect swamps out the direct beam. That is, there are few of the photons entering the water that are actually due to the direct solar beam, as is understandable within the context of Fresnel's law; the dominant source of light is diffuse skylight which represents an average of direct solar beams from 0 to 90 degrees. This effect has not previously been reported since much of our previous understanding comes from field data which is limited by the instrument technology which takes finite time to make measurements. During this time interval, the lighting conditions can change rapidly. It is difficult to measure values of  $k$  over large depths and for instantaneous solar positions when the sun is low in the sky. Such an effect is important to take into consideration when one is calculating the total availability of energy over one day.

The change in  $K$  as a function of depth is illustrated in Figures 22 and 23. Such calculations provide previously unavailable insight into depth dependence of  $K$ . For instance, Figure 23 shows three different wavelengths at several solar zenith angles. It should be noted that the spread between the 10 degree and the 60 degree curves decreases with depth, demonstrating that  $K$  approaches an asymptotic value at great depths which is wholly independent of the input radiance distribution.

The dependence of  $K$  on solar zenith angle is seen to be small here, agreeing with previous observations (Baker and Smith, 1979) that  $K$  is quasi-inherent for this type water. Baker and Smith fit a straight line through the log of the downwelling irradiance measurements to obtain  $K_d$  and as such the single value of  $K_d$  may be seen to be an average of  $K_d$  over the top 7-10 meters of the water column. Close scrutiny of the curves reveals that the asymptotic value of  $K_d$ , known as  $K_{\infty}$ , is reached extremely rapidly, as early as 4-5 meters depth. Thus, the average computed by Baker and Smith to represent  $K_d$



is swamped out by  $k_d$ , which is of course independent of solar zenith angle. This explains the "quasi-inherent" nature of  $k_d$  as reported previously.

It is now important to note that for 80 degrees, the asymptotic value is reached almost immediately. This suggests that scientists taking measurements in the field would do well to take data for low sun positions, in order to measure directly this highly important parameter.

The sensitivity of the model to  $Y$  is very small when a dry desert atmosphere was used compared with a coastal ocean atmosphere. It is only at low sun angles approaching 80 degrees that the atmospheric component ratio is found to have more than a 3 per cent influence on the resultant apparent optical properties. It is also found that  $K$  is relatively insensitive to wavelength variation in  $\rho$ , especially at the surface where the effect is less than 1 percent.

TABLE 1. TANK STUDY WAFER TYPES

#	file	CLAY		DOM		date
		gm	ppm	gm	mg/l	
1/	1	0	0	0	0	7oct82
2/	4	25	2.16	0	0	8oct82
3/	5	50	4.31	0	0	
4/	6	75	6.47	0	0	
5/	8	125	10.78	0	0	9oct82
6/	10	175	15.09	0	0	
7/	11	225	19.40	0	0	
8/	12	275	23.71	0	0	
9/	13	0	0	0	0	13oct82
10/	14	75	6.47	0	0	
11/	16	75	6.47	2	0.17	14oct82
12/	17	75	6.47	5	0.40	
13/	18	75	6.47	10	0.86	
14/	19	75	6.47	15	1.29	
15/	20	75	6.47	20	1.72	
16/	21	75	6.47	40	3.45	

Reproduced from  
best available copy



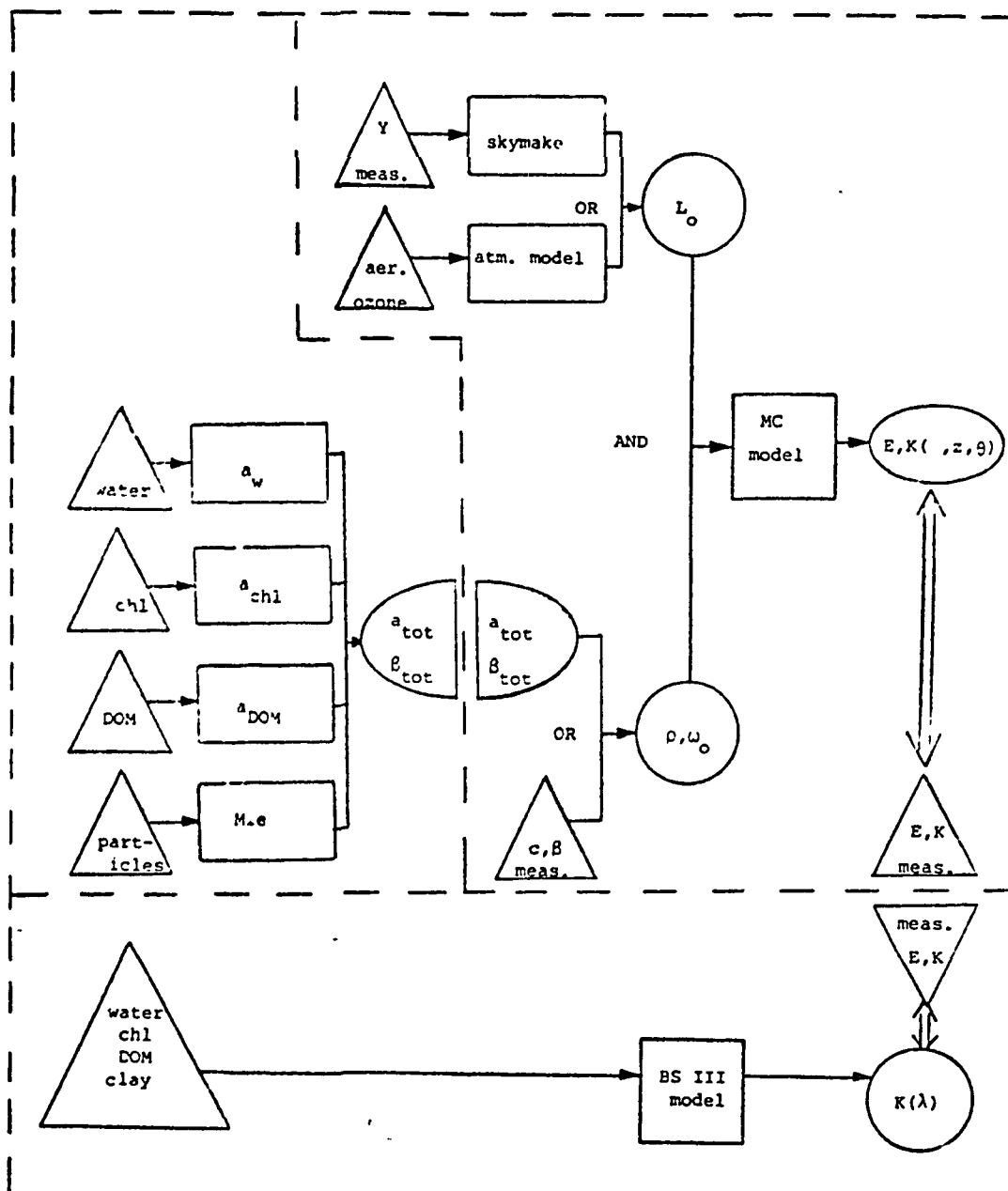


Figure 1. Relationships between experimental field data and computer models.

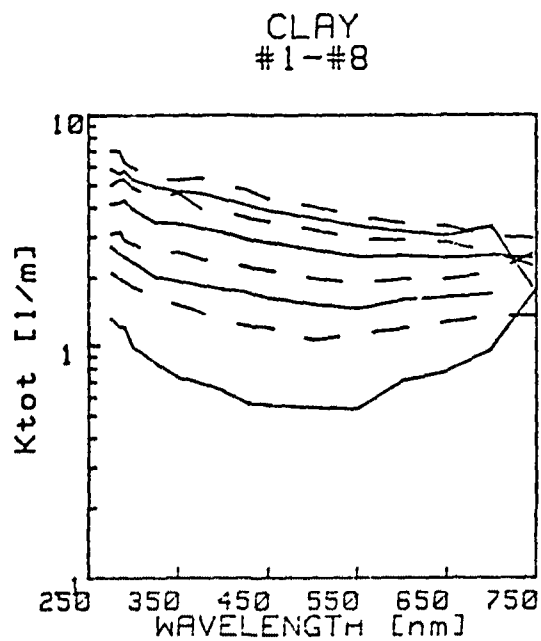


Figure 2. The spectral light attenuation in each of the Clay Group water types #1-#8 listed in Table 1.

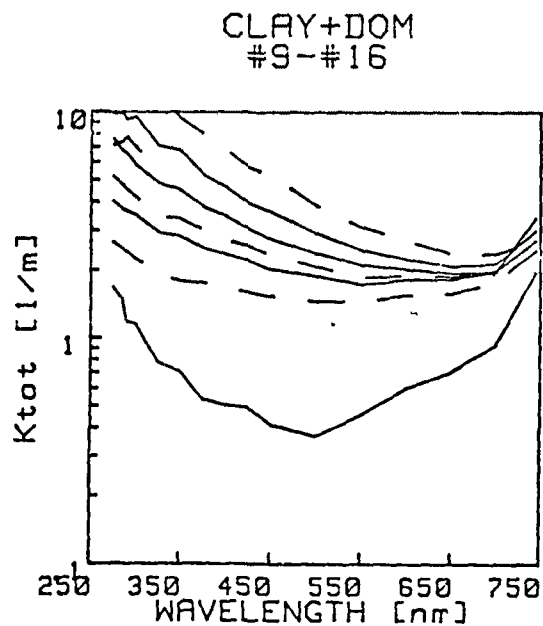


Figure 3. The spectral light attenuation in each of the DOM Group water types #9-#16 listed in Table 1.

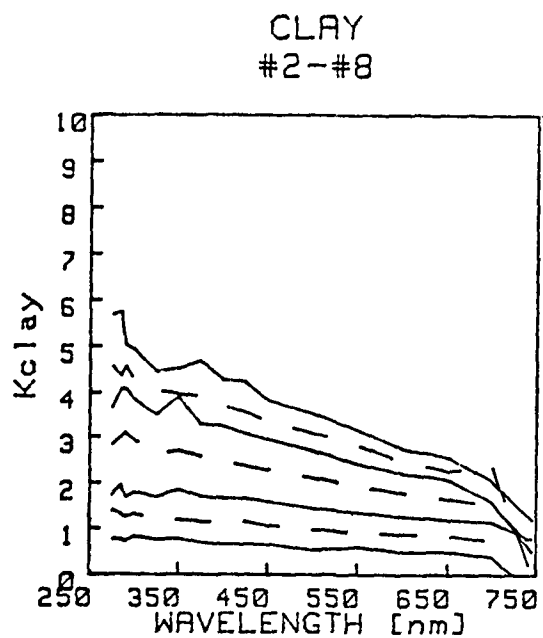


Figure 4. The spectral  $K_{clay}$  component for each of the Clay Group water types #2-#8 listed in Table 1.

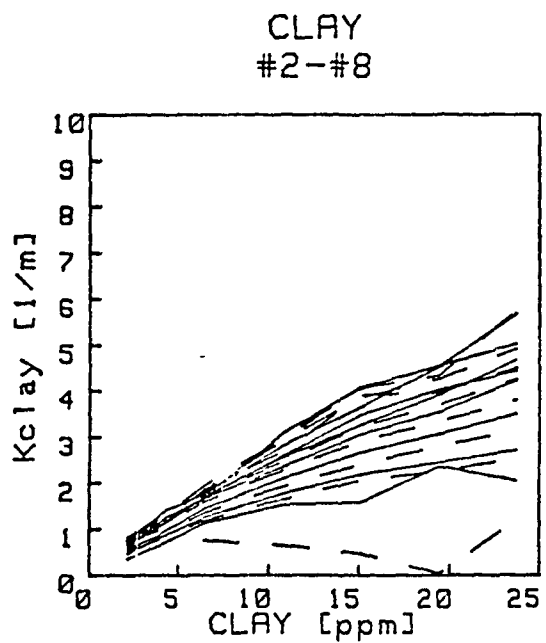


Figure 5. The  $K_{clay}$  component for the wavelength range from 275 nm to 745 nm.

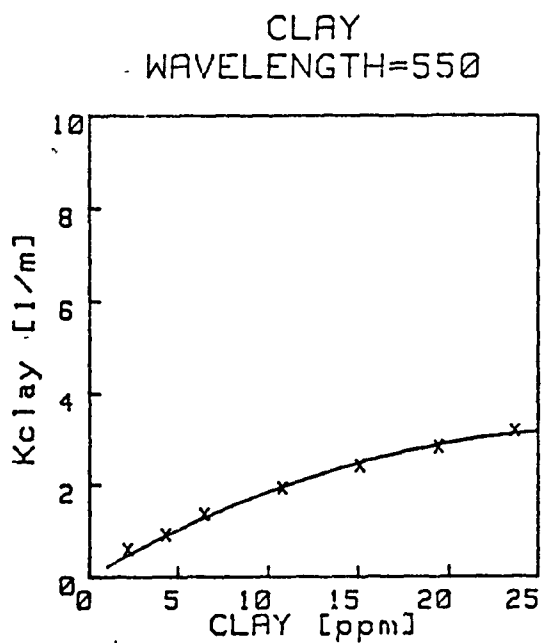


Figure 6. The Kclay component for the wavelength 550 nm for a range of clay (ppm) where the x's are experimental data and the line is a polynomial fit.

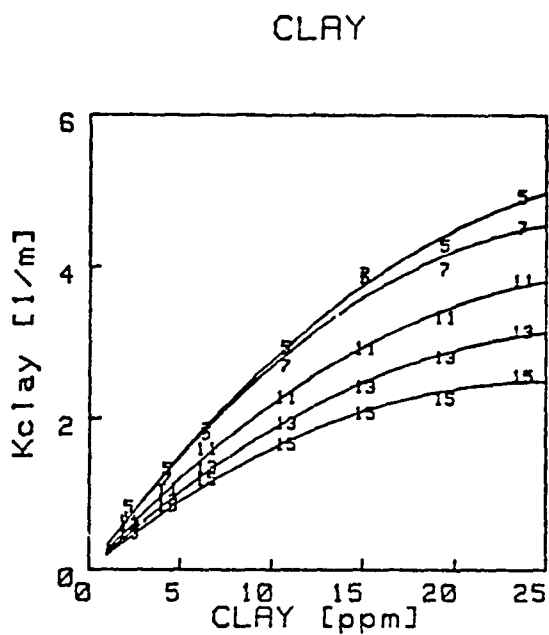


Figure 7. The Kclay component for five wavelengths where 5=300 nm, 11=450 nm, 13=550 nm, and 15=650 nm where these points represent data and the solid line is the model fit.

DOM  
#11-#16

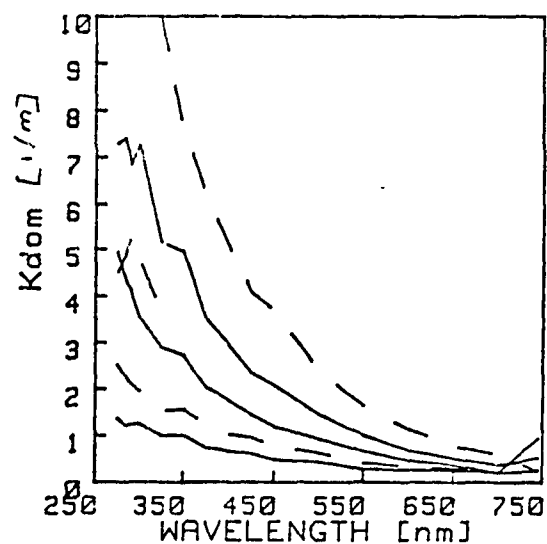


Figure 8. The spectral  $K_{dom}$  component (with scattering material still present; see text) for a DOM Group water types #11-#16 listed in Table 1.

DOM  
#11-#16

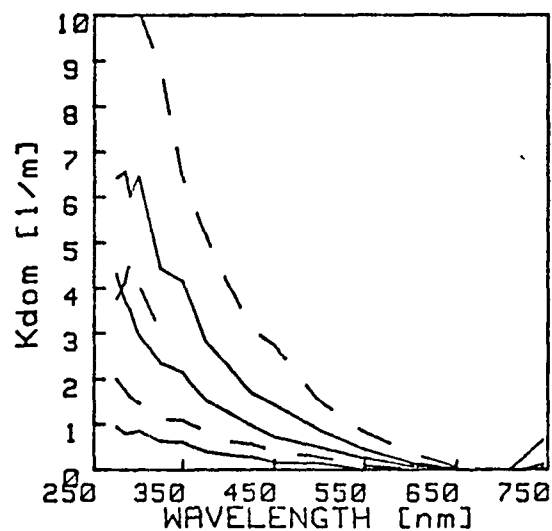


Figure 9. The spectral  $K_{dom}$  component for the DOM Group water types #11-#16 listed in table 1.

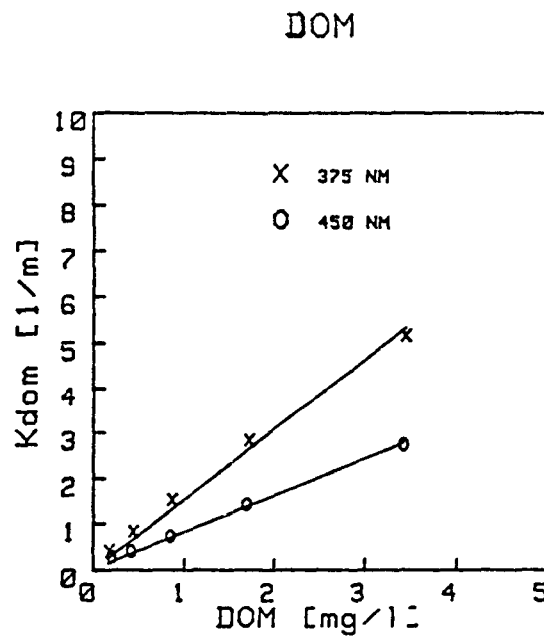


Figure 10. The  $K_{dom}$  component for two wavelengths where the points are data and the solid line is a fit.

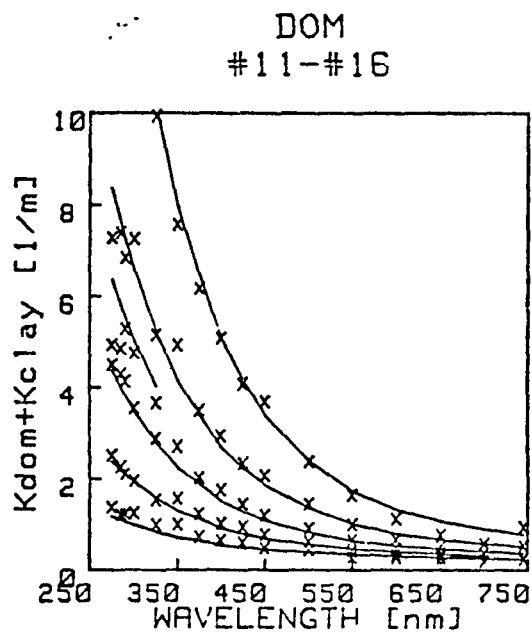


Figure 11. The spectral ( $K_{dom} + K_{clay}$ ) component where the x's are data and the line is the model fit.



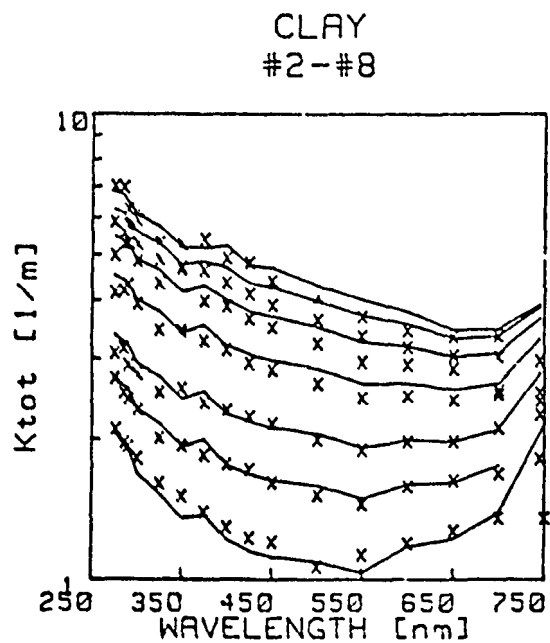


Figure 12. The spectral Ktot data points and analytic model fit as solid lines for the Clay Group.

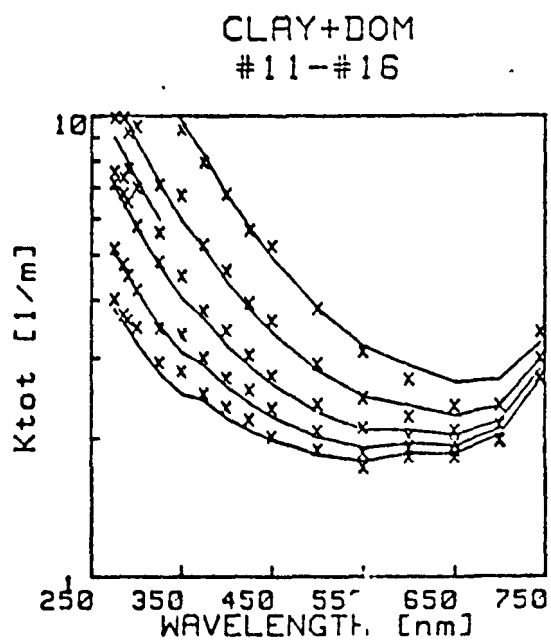


Figure 13. The spectral Ktot data points and analytic model fit as solid lines for the DOM Group.

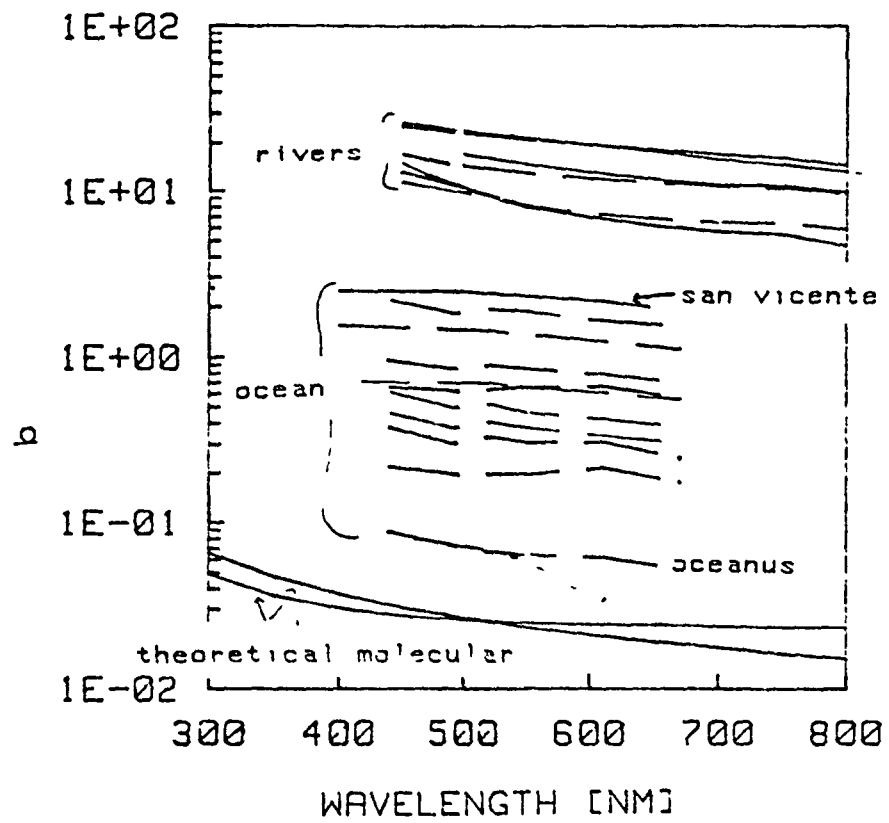


Figure 14. The total scattering  $b$  for a variety of water types from molecular scattering to clear water to ocean to river.

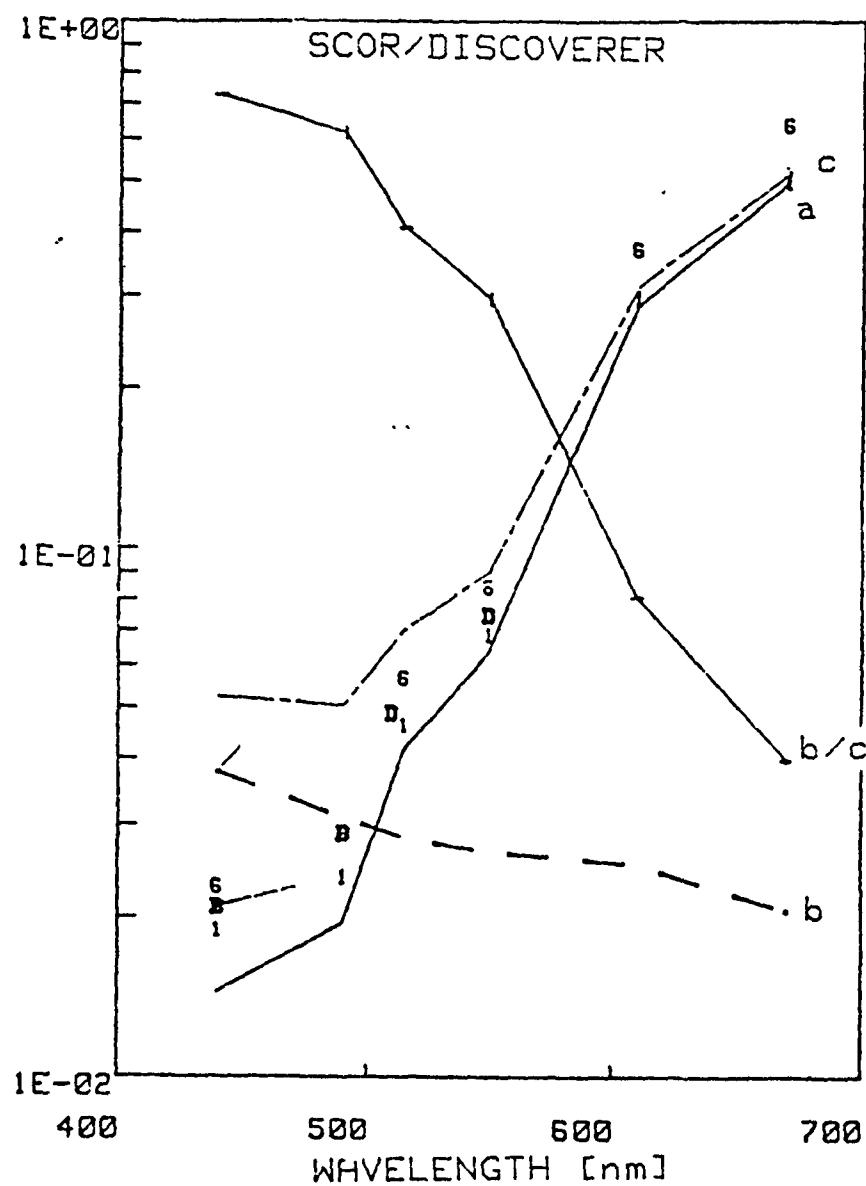


Figure 15. The spectral  $a$  (solid line),  $b$  (dashed line),  $c$  (dash dotted line), and  $b/c$  (notched line) for SCOR Discoverer station 21 Sargasso Sea waters. The  $D$  points are the field data measurements of total diffuse attenuation coefficient whereas the  $1, 6$  are the Monte Carlo calculations of  $K$  for 10 degrees and 60 degrees sun angles.

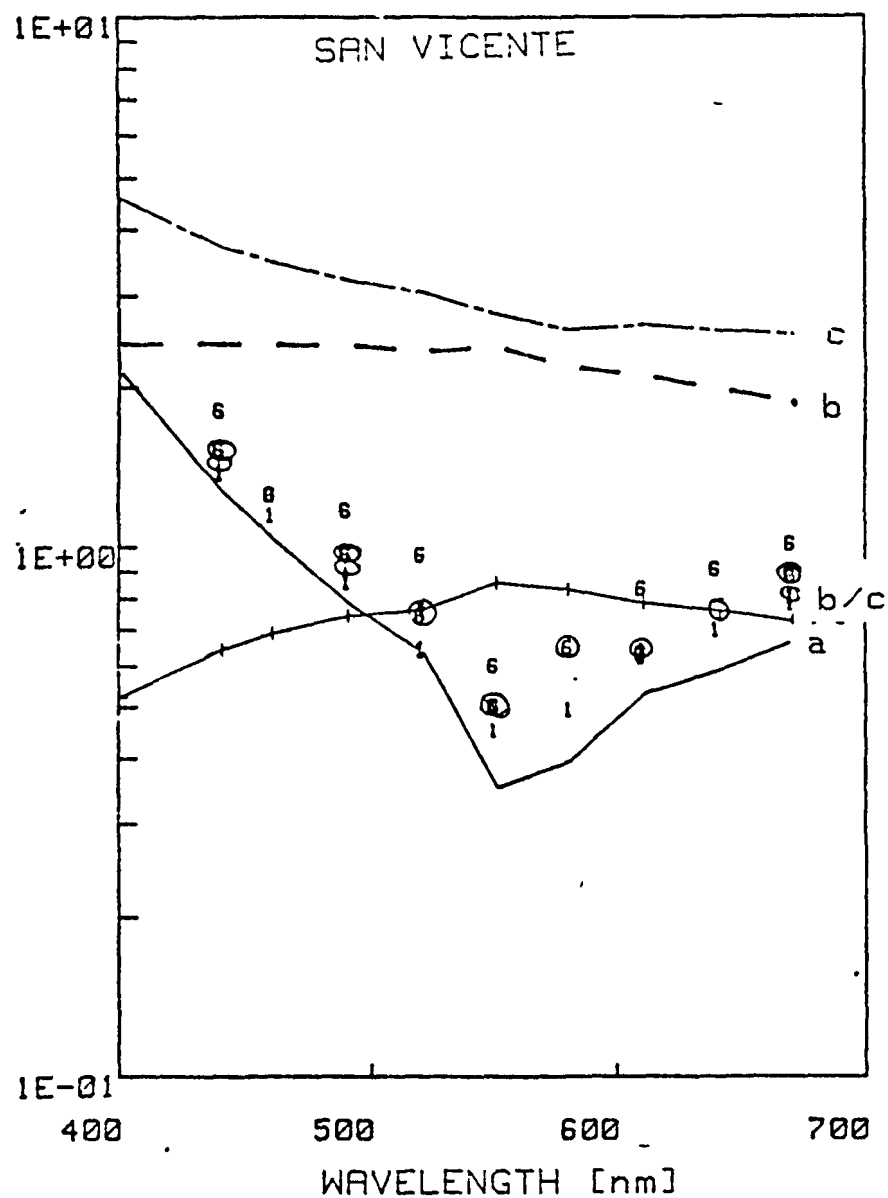


Figure 16. The a (solid line), b (dashed line), c (dash dotted line) and b/c (notched line) for San Vicente waters. The circled 1,6 points are the field measurements of total diffuse attenuation coefficients for sun angles 10 degrees and 60 degrees whereas the 1,6 points are the Monte Carlo predictions.

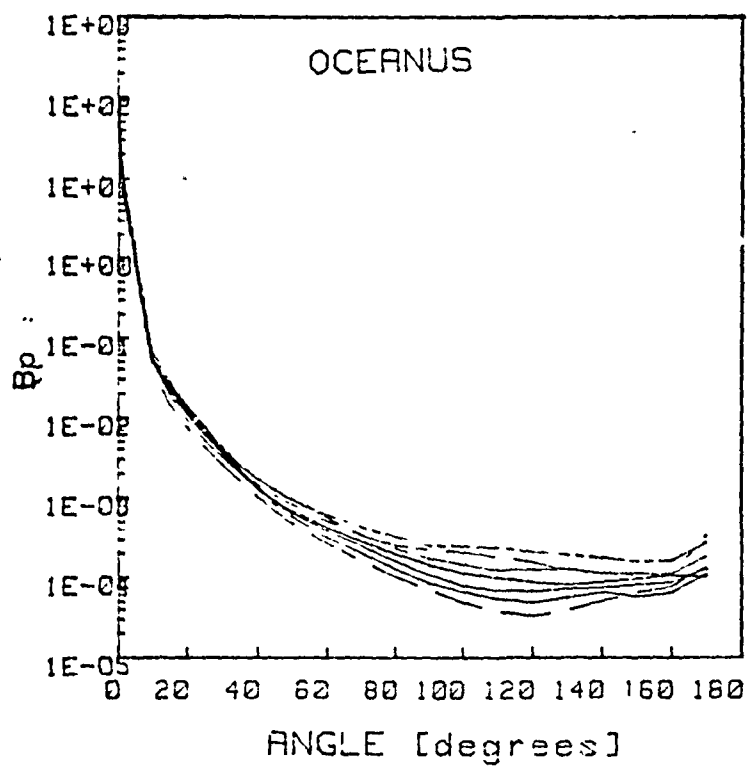


Figure 17. The particle volume scattering function for fairly clear ocean water (Oceanus cruise station 4) for wavelengths 440 nm, 490 nm, 520 nm, 610 nm, and 670 nm.

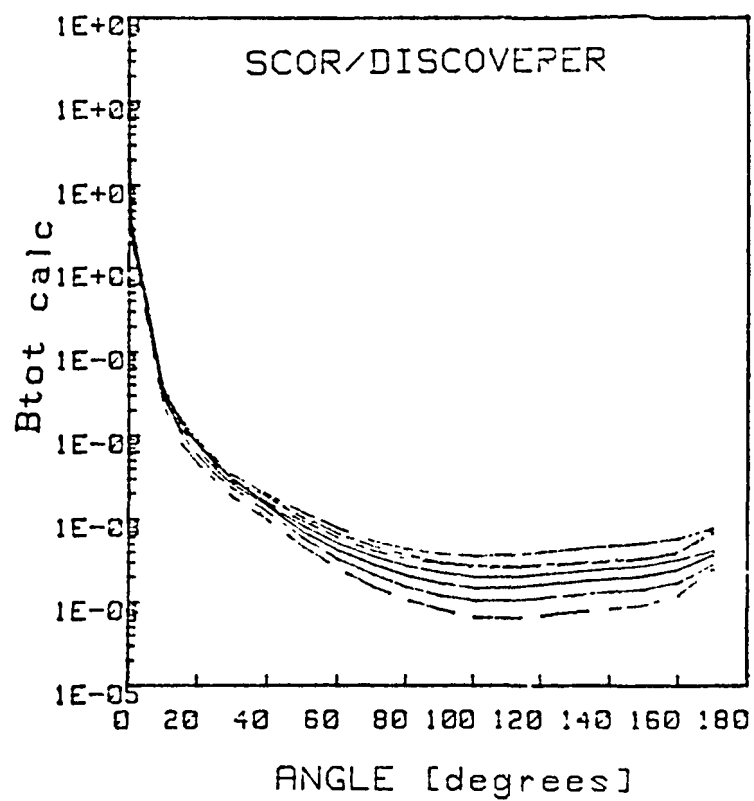


Figure 18. The calculated total volume scattering function for very clear ocean water (SCOR Discoverer station 21) for wavelengths 440 nm, 490 nm, 520 nm, 610 nm, and 670 nm.

# BSIII MODEL

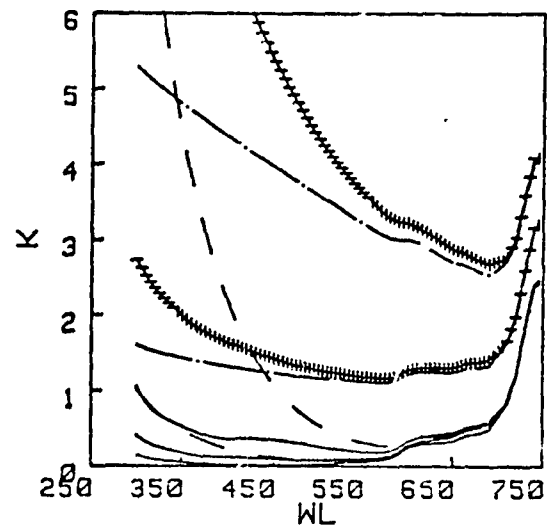


Figure 19. The Baker-Smith III component model prediction of spectral  $K_{tot}(\lambda)$  for a range of Chlorophyll, dissolved organic material and clay. The following explains the composition.

line	solid			dashed		dashed dot		hatched	
chl	0	.5	5.	0	0	0	0	.5	5
DOM	0	0	0	.5	5.	0	0	.5	5
clay	0	0	0	0	0	5	25	5	25

# SAN VICENTE DIRECT

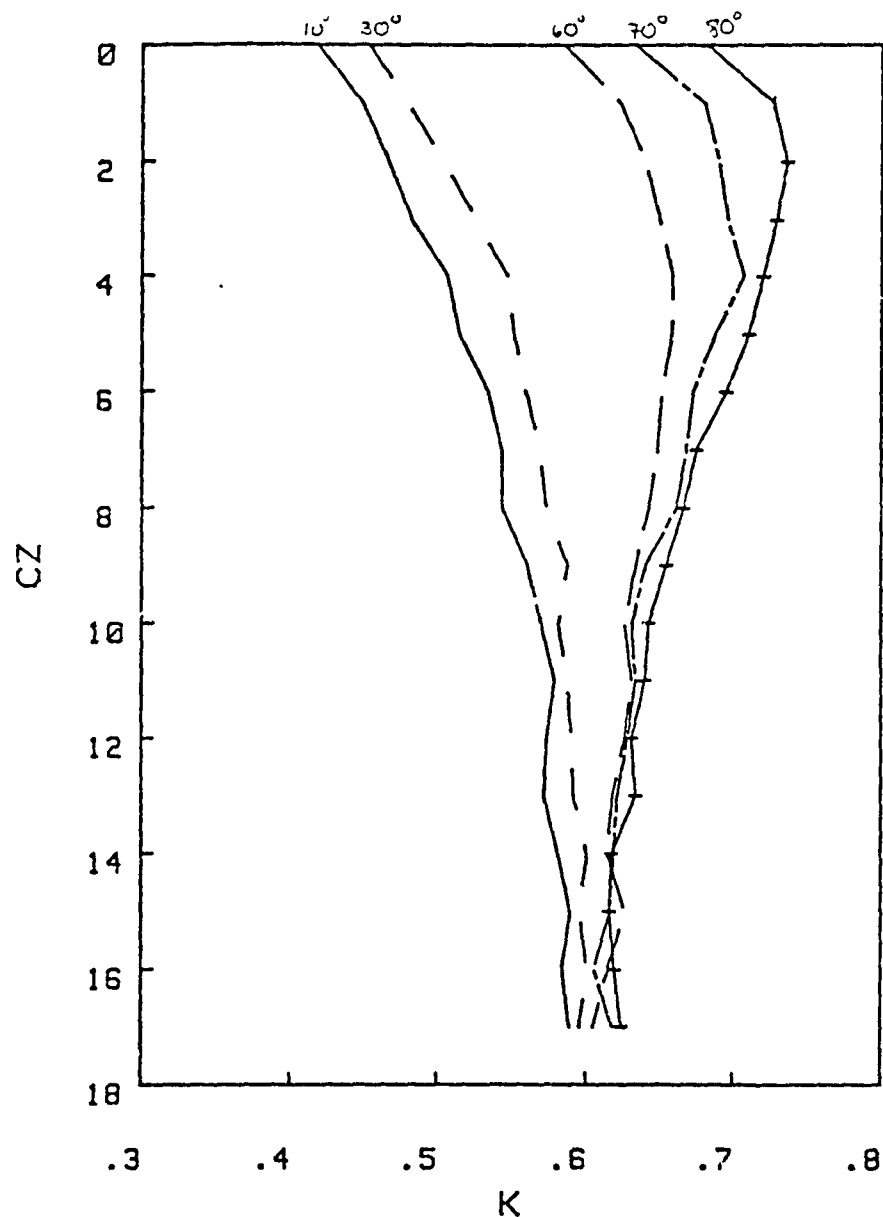


Figure 20. The Monte Carlo calculation of  $K(\lambda, z, 0)$  for wavelength 550 nm for sun angles 10, 30, 60, 70, 80 degrees plotted versus optical depths cz when using only a direct beam input to the water column.



# SAN VICENTE

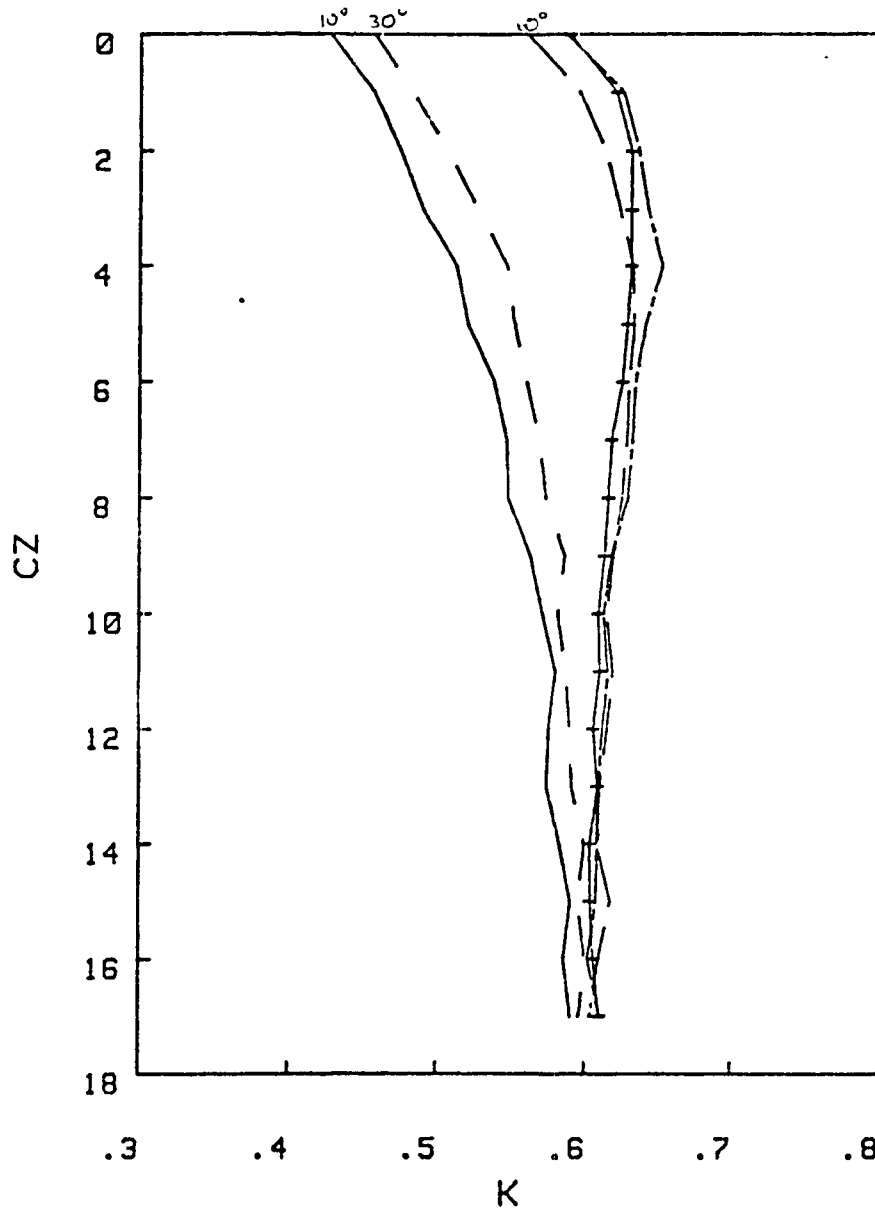


Figure 21. The Monte Carlo calculation of  $K(\lambda, z, 0)$  for wavelength 550 nm for sun angles 10, 30, 60, 70, 80 degrees plotted versus optical depths  $CZ$  when using both a direct and a diffuse input to the water column.

# DISCO

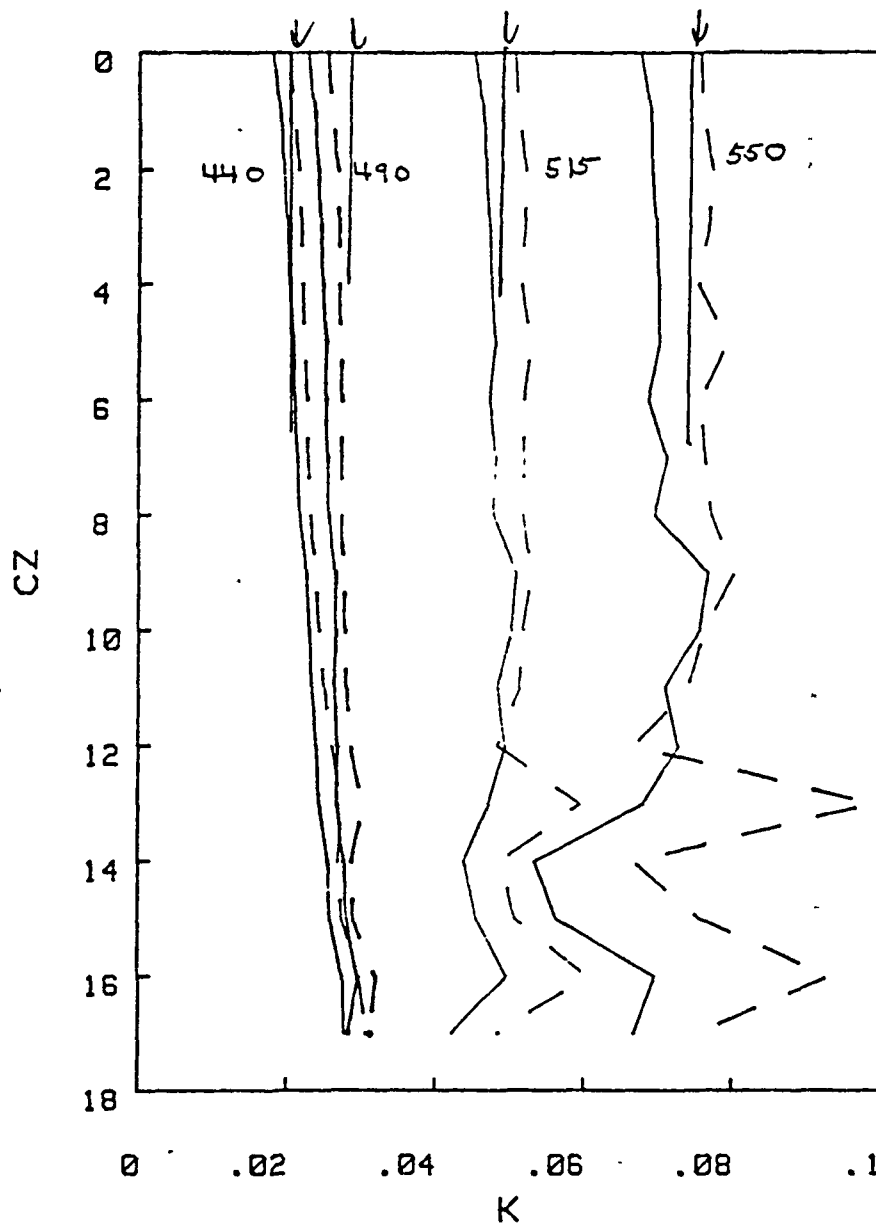


Figure 22. The Monte Carlo calculation of  $K(\lambda, z, 0)$  for clear waters of SCOR Discoverer for sun angle 10 degrees (solid line) and 40 degrees (broken line) for wavelengths 440 nm, 490 nm, 515 nm, and 550 nm. The straight line superimposed is the field measured value which is average for the day.

# SAN VICENTE

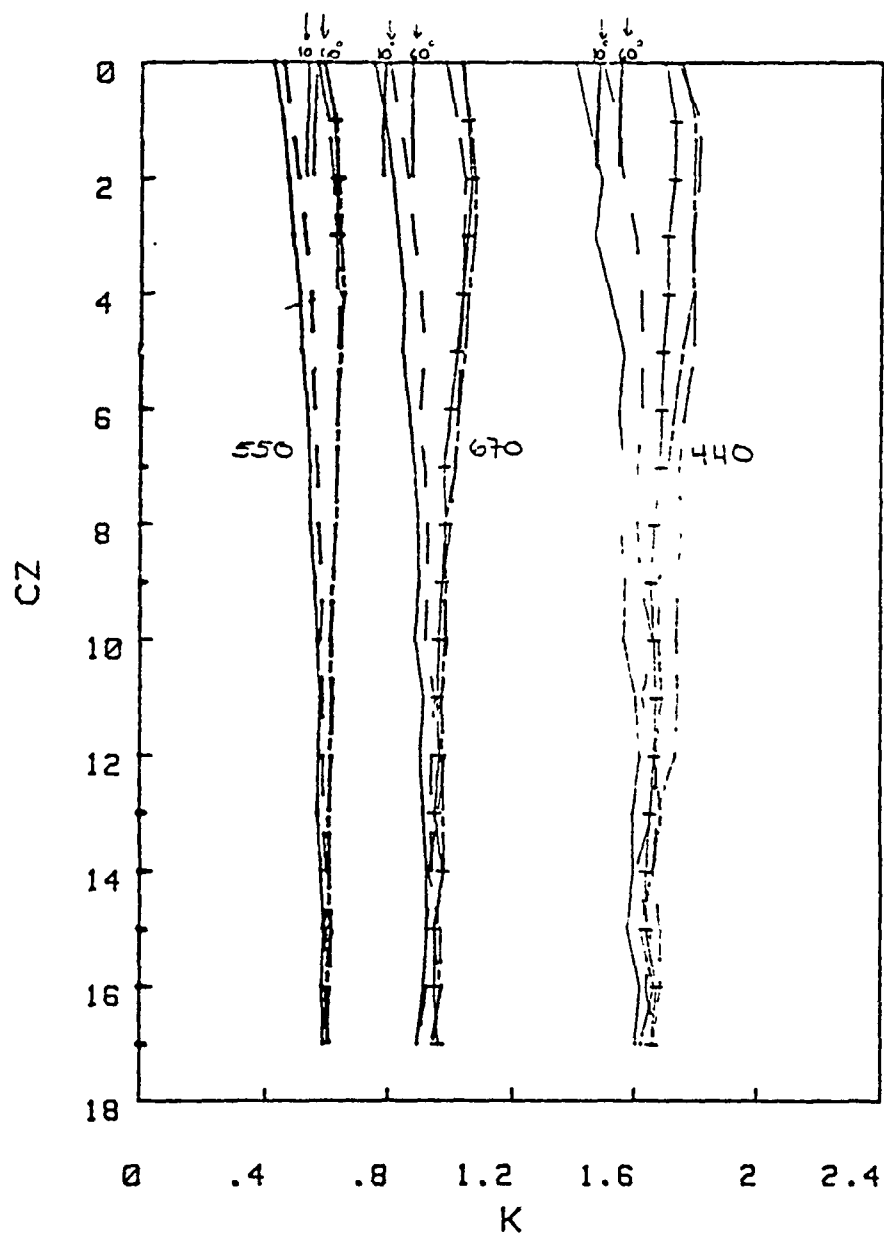


Figure 23. The Monte Carlo calculation of  $K(\lambda, z, 0)$  for San Vicente waters for sun angles 10, 30, 60, 70, 80 degrees for wavelengths 440 nm, 550 nm, and 670 nm. The straight lines superimposed are the field measured values for 10 and 60 degree sun angles.

## REFERENCES

- Baker, K.S. and R.C. Smith (1979). Quasi-innermost characteristics of the diffuse attenuation coefficient for irradiance. *SPIL*, Vol. 208, Ocean Optics VI.
- Baker, K.S., R.C. Smith, and A.E.S. Green (1980). Middle ultraviolet radiation reaching the ocean surface. *Photochem. Photobiol.*, 32:367-374.
- Baker, K.S. and R.C. Smith (1982): Bio-optical classification and model of natural waters II. *Limnol. Oceanogr.* 27(3) 500-509.
- Bice, K.L. and S.C. Clement (1981): Mineralogical, optical, geochemical and particle size properties of four sediment samples for optical physics research. NASA Contract Report 165663.
- Chapman, R.S. (1977): Particle size and x-ray analysis of feldspar, calvert, ball and jordan soils. NASA tech. memorandum, NASA TM x-73941.
- Dave, J.V. (1968): Subroutines for computing the parameters of the electromagnetic radiation scattered by a sphere. IBM Report 320-3237, IBM, Federal Systems Division, 18100 Frederick Pike, Gaithersburg, MD 20760.
- Dave, J.V. (1972) Development of programs for computing characteristics of ultraviolet radiation. IBM Tech. Report. IBM, Federal Systems Division, 18100 Frederick Pike, Gaithersburg, MD 20760.
- Green, A.E.S., T. Sawada and E.P. Shettle (1974). The middle ultraviolet reaching the ground. *Photochem. Photobiol.*, 19 251-259.
- Gordon, H.R. (1975): Diffuse reflectance of the ocean: some effects of vertical structure. *Appl. Opt.*, 14:2892-2895.
- Gordon, H.R., O.B. Brown, and M.M. Jacobs (1975): Computed relationships between the innermost and apparent optical properties of a flat homogeneous ocean. *Appl. Opt.*, 14:417-427.
- Gordon, H.R. (1977). Albedo of the ocean atmosphere system, influence of sea foam. *Appl. Opt.*, 16:2257-2260.
- International Association of Meteorology and Atmospheric Physics (IAMAP) radiation commission. Standard procedures to compute atmospheric radiative transfer in a scattering atmosphere. (1977), NCAR, Boulder, CO 80307.
- Kirk, J.T.O. (1981): A Monte Carlo procedure for simulating the penetration of light into natural waters. Division of Plant Industry Technical Paper No. 36, Commonwealth Scientific and Industrial Research Organization, Australia.
- Kirk, J.T.O. (1981): A Monte Carlo study of the nature of the underwater light field in, and the relationships between, optical properties of turbid yellow waters. *Australian Journ. Mar. Freshwater Res.*, 32:517-532.
- Mie, G. (1908): *Annul. Physik.*, 25:377.

- Miller, G.C. and R.G. Zepp (1978): Effects of suspended sediments on photolysis rates of dissolved pollutants. *Water Res.* 13:453-459.
- Petzold, T.J. (1972): Volume scattering functions for selected ocean waters. University of California at San Diego, Scripps Institution of Oceanography, Ref. 77-78.
- Plass, G. and G. Kattawar (1969). Radiative transfer in an atmosphere-ocean system. *Appl. Opt.*, 8:455-466.
- Plass, G. and G. Kattawar (1972): Monte Carlo calculations of radiative transfer in the earth's atmosphere-ocean system: I flux in the atmosphere and ocean. *Jour. Phys. Oceanogr.*, 2:139-145.
- SCOR Data Report of the Discoverer Expedition May 1970 (1973). J.E. Tyler (ed.), University of California at San Diego, SIO Ref. 73-16 (1000 pages).
- Poole, L.R., W. Esaias, J. Campbell (in press). A semi-analytic Monte Carlo radiative transfer model for oceanographic lidar systems.
- Preisendorfer, R.W., 1976: *Hydrologic Optics*, vol. I-VI, U.S. Dept. of Commerce, NOAA.
- Smith, R.C. and K.S. Baker (1978a). The bio-optical state of ocean waters and remote sensing. *Limnol. Oceanogr.*, 23(2):247-259.
- Smith, R.C. and K.S. Baker (1978b). Optical classification of natural waters. *Limnol. Oceanogr.*, 23(2):260-267.
- Smith, R.C., R.L. Ensminger, R.W. Austin, J.D. Bailey, G.D. Edwards, (1979): Ultraviolet submersible spectroradiometer. *Proceedings of the Society of Photo-optical instrumentation engineers (SPIE). Ocean Optics VI*, Vol. 208:127-140.
- Smith, R.C. and K.S. Baker (1981): Optical properties of the clearest natural waters (200-800nm). *Applied Optics*, 20:177-184.
- Wiscombe, W.J. (1979). Mie scattering calculations. advanced techniques and vector-space computer codes. NCAR Tech. note NCAR/TN-140+STR.
- Zepp, K.G. and P.F. Schlotzhauer (1981): Comparison of photochemical behavior of various humic substances in water: III. Spectroscopic properties of humic substances in *Chemosphere*, vol. 10, 5:479-486. Pergamon Press.

IMPORTANT NOTICE

Effective on orders received June 1, 1985, the following  
NTIS shipping and handling charges apply:

U.S., Canada, Mexico, - ADD \$3 per TOTAL ORDER

All other Countries - ADD \$4 per TOTAL ORDER

Exceptions - Does NOT apply to:

ORDERS REQUESTING NTIS RUSH HANDLING

ORDERS FOR SUBSCRIPTION OR STANDING ORDER PRODUCTS ONLY

NOTE: Each additional delivery address on an order requires a separate  
shipping and handling charge.

END